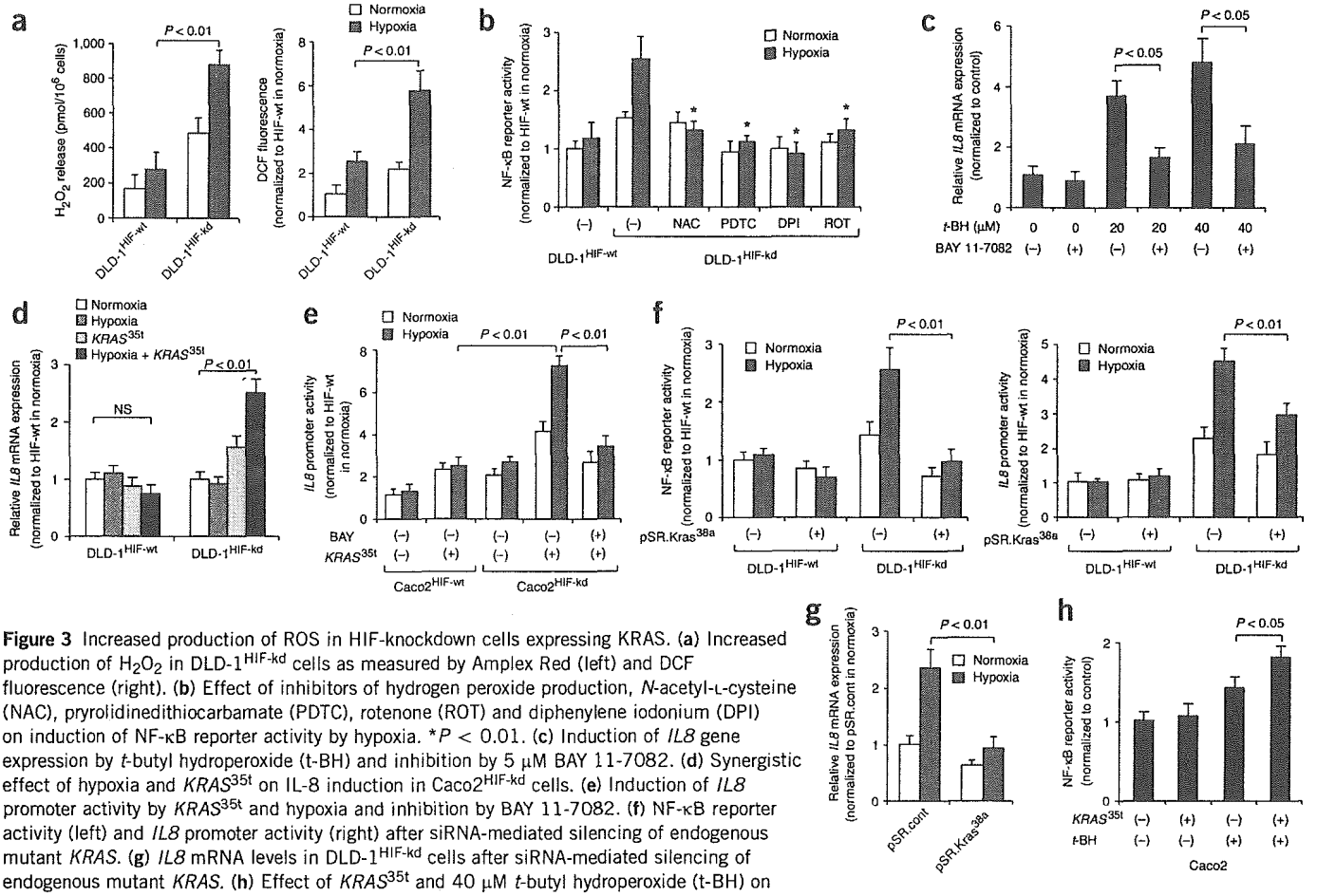

Figure 3 Increased production of ROS in HIF-knockdown cells expressing KRAS. (**a**) Increased production of H_2O_2 in DLD-$1^{HIF\text{-}kd}$ cells as measured by Amplex Red (left) and DCF fluorescence (right). (**b**) Effect of inhibitors of hydrogen peroxide production, *N*-acetyl-L-cysteine (NAC), pryrolidinedithiocarbamate (PDTC), rotenone (ROT) and diphenylene iodonium (DPI) on induction of NF-κB reporter activity by hypoxia. $^*P < 0.01$. (**c**) Induction of *IL8* gene expression by *t*-butyl hydroperoxide (t-BH) and inhibition by 5 μM BAY 11-7082. (**d**) Synergistic effect of hypoxia and $KRAS^{35t}$ on IL-8 induction in Caco$2^{HIF\text{-}kd}$ cells. (**e**) Induction of *IL8* promoter activity by $KRAS^{35t}$ and hypoxia and inhibition by BAY 11-7082. (**f**) NF-κB reporter activity (left) and *IL8* promoter activity (right) after siRNA-mediated silencing of endogenous mutant *KRAS*. (**g**) *IL8* mRNA levels in DLD-$1^{HIF\text{-}kd}$ cells after siRNA-mediated silencing of endogenous mutant *KRAS*. (**h**) Effect of $KRAS^{35t}$ and 40 μM *t*-butyl hydroperoxide (t-BH) on NF-κB reporter activity in Caco2 cells.

online). Furthermore, we observed the stimulatory effect of oncogenic *KRAS* on NF-κB in hypoxic conditions or in the presence of ROS (**Figs. 3d,h**). Collectively, these studies indicate that IL-8 can be induced in hypoxia through the activation of NF-κB in the absence of HIF-1, and that oncogenic *KRAS* can further stimulate NF-κB in hypoxic conditions to upregulate this alternative angiogenic pathway.

Finally, we sought to determine the functional significance of IL-8 production in HIF-1–deficient tumors. The observation that DLD-$1^{HIF\text{-}kd}$ xenografts showed a marked inflammatory infiltrate (**Fig. 1c**) was consistent with a functional role for IL-8, a potent neutrophil chemokine[18]. Intraperitoneal administration of the IL-8 neutralizing antibody MAB208 resulted in complete regression of 25% of DLD-$1^{HIF\text{-}kd}$ xenografts, and among the other detectable DLD-$1^{HIF\text{-}kd}$ tumors, there was a 61.3% reduction in tumor volume ($P < 0.01$) and 61.8% reduction in tumor weight ($P < 0.01$) compared to tumors treated with control IgG (**Fig. 4a,b**). In contrast, there was only a 24.8% ($P = 0.28$) and 15.6% ($P = 0.35$) reduction in tumor volume and weight, respectively, in DLD-$1^{HIF\text{-}wt}$ xenografts. Although treatment with MAB208 resulted in a decrease in the Ki-67 labeling index and increase in apoptosis in the DLD-$1^{HIF\text{-}kd}$ xenografts (**Fig. 4c**), *in vitro* studies showed that MAB208 did not directly inhibit tumor cell growth (**Fig. 4d**). Rather, treatment with MAB208 resulted in a considerable inhibition of angiogenesis. The microvessel density in DLD-$1^{HIF\text{-}kd}$ xenografts was reduced 46.5% ($P < 0.001$) compared to a 14.5% reduction ($P = 0.11$) in DLD-$1^{HIF\text{-}wt}$ xenografts (**Fig. 4e**). Confocal microscopy of tumor sections after lectin perfusion verified that vascular integrity was compromised in DLD-$1^{HIF\text{-}kd}$ xenografts treated with MAB208 (**Fig. 4e**). In addition to reduced vessel number, the vessels were markedly narrowed and fragmented. Specifically, the mean vessel diameter fell from 22.4 μm to 5.9 μm ($P = 0.0002$) when we treated DLD-$1^{HIF\text{-}kd}$ xenografts with MAB208, but there was no change in the DLD-$1^{HIF\text{-}wt}$ xenografts (26.5 μm versus 24.8 μm with MAB208; not significant). Neutralization of both IL-8 and VEGF in DLD-$1^{HIF\text{-}kd}$ xenografts had an additive effect on the inhibition of tumor growth (**Fig. 4f**), showing that each factor can regulate tumorigenesis independently.

In summary, we have shown that HIF-1α deficiency in colon cancer cells can inhibit proliferation and overall growth, but not angiogenesis. There are conflicting reports of the role of HIF-1 in tumor cell proliferation. *Hif1a*$^{-/-}$ embryonic stem cell–derived teratocarcinomas show reduced as well as increased growth[2,20]. Among human tumors, overexpression of HIF-1α has been associated with improved survival in individuals with head and neck cancers[21] and HIF-1 can inhibit the growth of renal carcinoma cells[22]. This may be mediated through the induction of the cell-cycle inhibitors p21 and p27 (ref. 23). It has been speculated that HIF-1 may have intrinsic functions to either promote or inhibit tumor growth that depends upon the cellular context[24]. The preservation of angiogenesis in our model can be explained by persistent expression of VEGF as well as induction of the proangiogenic factor, IL-8. IL-8 was stimulated by ROS-mediated activation of NF-κB, and this was enhanced by oncogenic *KRAS*. Neutralization of IL-8 in HIF-1–deficient tumors led to a substantial inhibition of

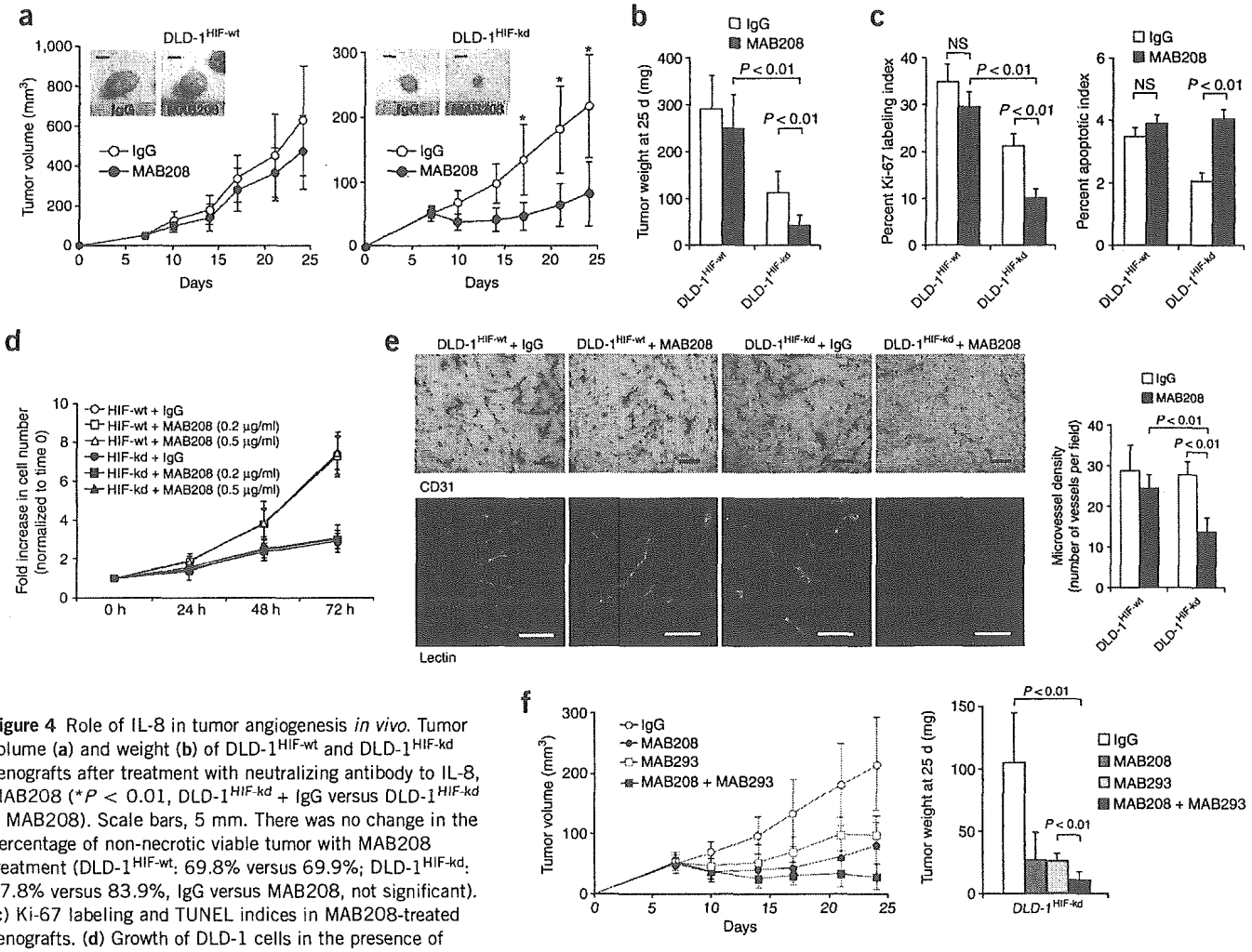

Figure 4 Role of IL-8 in tumor angiogenesis *in vivo*. Tumor volume (**a**) and weight (**b**) of DLD-1$^{HIF\text{-}wt}$ and DLD-1$^{HIF\text{-}kd}$ xenografts after treatment with neutralizing antibody to IL-8, MAB208 (*$P < 0.01$, DLD-1$^{HIF\text{-}kd}$ + IgG versus DLD-1$^{HIF\text{-}kd}$ + MAB208). Scale bars, 5 mm. There was no change in the percentage of non-necrotic viable tumor with MAB208 treatment (DLD-1$^{HIF\text{-}wt}$: 69.8% versus 69.9%; DLD-1$^{HIF\text{-}kd}$: 87.8% versus 83.9%, IgG versus MAB208, not significant). (**c**) Ki-67 labeling and TUNEL indices in MAB208-treated xenografts. (**d**) Growth of DLD-1 cells in the presence of MAB208 under hypoxic conditions. (**e**) Blood vessels visualized by CD31 immunohistochemistry (upper; scale bar, 100 μm) and lectin perfusion (lower; scale bar, 50 μm). Narrow and fragmented vessels are present in DLD-1$^{HIF\text{-}kd}$ + MAB208. (**f**) Growth of DLD-1$^{HIF\text{-}kd}$ xenografts when treated with a neutralizing VEGF antibody (MAB293) and/or a neutralizing antibody to IL-8 (MAB208). In these xenografts, the percentage of viable non-necrotic tumor fell slightly to 74.7% from 87.8% in mice that received control antibody only ($P = 0.1$).

angiogenesis and tumor growth. Studies of lung cancer cells harboring a *KRAS* mutation have also shown a pivotal role for IL-8 in tumor angiogenesis[25]. Collectively, these findings highlight the complex role of HIF-1α in colorectal tumorigenesis, the diversity of pathways used by tumors to stimulate angiogenesis, and the potential for combination antiangiogenic regimens that target both HIF-1 and IL-8.

METHODS

Cell lines. We stably transfected DLD-1 and Caco2 cells (ATCC) with HIF-1α–specific siRNA constructs (pSuper.retro, OligoEngine), pSR.HIF-1α1470 or pSR.HIF-1α2192 (ref. 10). Three independent DLD-1 clones stably expressing pSR.HIF-1α1470 and two independent clones expressing pSR.HIF-1α2192 showed similar responses to hypoxia with respect to induction of NF-κB and IL-8. In a pilot xenograft study, growth, microvascular density, VEGF and IL-8 levels were similar between a pSR.HIF-1α1470 clone and pSR.HIF-1α2192 clone. Hypoxic conditions (1% O_2) were achieved with a sealed hypoxia chamber (Billups-Rothenberg) in serum-free UltraCulture medium (Cambrex)[10]. We performed transient transfections using Lipofectamine 2000 (Invitrogen).

Plasmid constructs. The IL-8 reporter[26], NF-κB reporter and phr-GFP-KRAS^{35t} plasmids have been described[27]. We performed site-directed mutagenesis to obtain the phr-GFP-KRAS^{38a} construct. We constructed pSuper.Kras^{38a} (pSR.Kras^{38a}) by subcloning the sequence 5′-GGAGCTGGTGACGTAGGCA-3′. For control siRNA, pSR.cont, we used the sequence 5′-GCGCGCTTTGTAG GATTCG-3′ (ref. 28). For mutations in *KRAS*, we used a numbering system in which position 1 is the A of the initiator ATG codon. *KRAS*^{38a} results in a Gly13Asp mutation and *KRAS*^{35t} results in a Gly12Val mutation.

Transfections and reporter assays. We cotransfected 0.1–0.2 μg of reporter constructs with 2 ng of pRL-CMV (Promega) and measured luciferase activity with the Dual Luciferase Reporter Assay System (Promega). We used pRL-null, a promoter-less *Renilla* construct, when we cotransfected cells with a KRAS expression vector[29]. We calculated the relative luciferase activity as the ratio of firefly/*Renilla* luciferase activity. The level of 'hypoxic induction' was the ratio between the relative luciferase activity in hypoxia to that in normoxia.

Xenograft tumor model. We injected 2 × 10^6 cells subcutaneously into the flanks of 6–8-week-old CD1 female nude mice (six mice per arm). We measured tumors with calipers and calculated volume as (length × width^2) × 0.5. We intraperitoneally administered neutralizing antibody to IL-8 (MAB208, clone 6217.111; R&D Systems) and/or VEGF (MAB293, R&D Systems) when tumors reached 5 mm. We injected 100 μg of MAB208 and/or 25 μg of MAB293 on days 7, 9, 11, 14, 16, 18, 21 and 23, before mice were

killed at day 25. To assess hypoxic regions, we intraperitoneally injected mice with 60 mg/kg pimonidazol hydrochloride (Hypoxyprobe-1, Chemicon), 1.5 h before killing. To visualize functional tumor microvessels, we intravenously injected 100 μg FITC-labeled tomato lectin (Vector Laboratories), and perfused the hearts of the mice with 4% paraformaldehyde. This protocol was approved by the Animal Care and Use Committee of the Massachusetts General Hospital.

Immunohistochemistry. We treated 5-μm sections from fresh frozen tumors with acetone and blocked endogenous peroxidase with 3% H_2O_2. We incubated the sections with a CD31-specific antibody, MEC13.3 (1:50; Pharmingen), overnight at 4 °C. We counted blood vessels in 5–10 random viable fields (magnification, ×200). To detect tumor hypoxia, we treated formalin-fixed sections with 0.01% pronase and incubated them with Hypoxpyrobe-1–specific antibody Mab1 (1:50; Chemicon). For other immunohistochemical studies, we fixed xenograft tissues in 10% neutral buffered formalin. We performed TUNEL staining with the ApoAlert DNA fragmentation detection kit (Clontech). We performed Ki-67 staining with the MIB-1 antibody (1:100; DAKO) and performed staining for Ser563-phosphorylated p65 (1:50; Cell Signaling).

Real-time PCR assay. We extracted RNA using the RNeasy kit (Qiagen) and performed quantitative reverse transcription PCR using the SuperScript III platinum Two-Step qRT-PCR Kit (Invitrogen). Primer sequences for *VEGF*, *IL8* and 18S RNA are available upon request. We used a fluorogenic SYBR Green and MJ research detection system for real-time quantification.

Immunoblotting. We performed immunoblot analysis for HIF-1α (clone 54, 1:250; Transduction Laboratories), HIF-2α (1:250, Novus), Glut-1 (GT-11A, 1:1000; Alpha Diagnostic International), VEGF (Ab-2, 1:40; Calbiochem), Ser563-phosphorylated p65 and total NF-κB p65 (1:1,000; both Cell Signaling), KRAS (F234, 1:200; Santa Cruz) and β-actin (AC15, 1 μg/ml; Sigma) after SDS-PAGE and electrophoretic transfer to polyvinylidene fluoride membranes[10].

ELISA. We assayed the levels of VEGF and IL-8 protein in conditioned medium and tissue lysates using specific ELISA kits (Quantikine, R&D Systems).

Microarray analysis. We performed sample preparation and processing procedures as described in the Affymetrix GeneChip Expression Analysis Manual. We hybridized the labeled cRNA samples to the complete Affymetrix human U133 GeneChip set (HG-U133A).

Hydrogen peroxide studies. We measured H_2O_2 using the Amplex Red Hydrogen peroxide Assay Kit and the CM-H2DCFDA reagent (both from Molecular Probes). We exposed cells to hypoxia for 10 h, and then switched culture medium to Krebs-Ringer phosphate buffer[30] containing 100 μM Amplex Red reagent and 0.2 U/ml horseradish peroxidase. After additional incubation in hypoxia for 1 h, we measured fluorescence in 96-well plates using Spectra MAX GEMINI XS microplate fluorometer (Molecular Devices). We also incubated cells with 10 μM CM-H2DCFDA for 30 min in RPMI without phenol red. We measured fluorescence in 96-well plates and normalized values to cell number. We added 20 or 40 μM *t*-butyl hydroperoxide (Sigma) to the culture media of DLD-1 cells every 30 min for 6 h and measured *IL8* mRNA using qRT-PCR.

Statistical analysis. We performed statistical analyses with a two-tailed, unpaired Student *t*-test.

Note: Supplementary information is available on the Nature Medicine website.

ACKNOWLEDGMENTS

We thank the following individuals for sharing these plasmids: C. Reinecker (IL-8 reporter construct), R. Xavier (NF-κB reporter construct, phr-GFP-K-ras^{Val12}) and D. Tenen (pRL-null). We also thank Y. Kamegaya, M. Takeda, M. Ii, E. di Tomaso, T. Padera, P. Au and R. Tyszkowski for assistance with tissue analysis. DNA microarray studies were performed at the DNA Microarray Core Facility at the Massachusetts General Hospital Cancer Center. Confocal microscopy was performed through the Imaging Core of the Center for Study of Inflammatory Bowel Diseases. This work was supported by US National Institutes of Health (NIH) research grant CA92594 to D.C.C. O.I. was supported by NIH grant CA104574, B.R.R. was supported by NIH grant CA098333, M.A.Z. was supported by von Hippel-Lindau Family Alliance, M.G. was supported by an American Gastroenterology Association student fellowship award, and E.-M.D. was supported by a postdoctoral fellowship award from the Deutsche Forschungsgemeinschaft.

COMPETING INTERESTS STATEMENT

The authors declare that they have no competing financial interests.

Received 10 June; accepted 2 August 2005
Published online at http://www.nature.com/naturemedicine/

1. Denko, N.C. *et al.* Investigating hypoxic tumor physiology through gene expression patterns. *Oncogene* **22**, 5907–5914 (2003).
2. Carmeliet, P. *et al.* Role of HIF-1alpha in hypoxia-mediated apoptosis, cell proliferation and tumour angiogenesis. *Nature* **394**, 485–490 (1998).
3. Pugh, C.W. & Ratcliffe, P.J. Regulation of angiogenesis by hypoxia: role of the HIF system. *Nat. Med.* **9**, 677–684 (2003).
4. Tang, N. *et al.* Loss of HIF-1alpha in endothelial cells disrupts a hypoxia-driven VEGF autocrine loop necessary for tumorigenesis. *Cancer Cell* **6**, 485–495 (2004).
5. Kung, A.L., Wang, S., Klco, J.M., Kaelin, W.G. & Livingston, D.M. Suppression of tumor growth through disruption of hypoxia-inducible transcription. *Nat. Med.* **6**, 1335–1340 (2000).
6. Semenza, G.L. Targeting HIF-1 for cancer therapy. *Nat. Rev. Cancer* **3**, 721–732 (2003).
7. Hurwitz, H. *et al.* Bevacizumab plus irinotecan, fluorouracil, and leucovorin for metastatic colorectal cancer. *N. Engl. J. Med.* **350**, 2335–2342 (2004).
8. Maxwell, P.H. *et al.* Hypoxia-inducible factor-1 modulates gene expression in solid tumors and influences both angiogenesis and tumor growth. *Proc. Natl. Acad. Sci. USA* **94**, 8104–8109 (1997).
9. Ryan, H.E. *et al.* Hypoxia-inducible factor-1alpha is a positive factor in solid tumor growth. *Cancer Res.* **60**, 4010–4015 (2000).
10. Mizukami, Y. *et al.* Hypoxia-inducible factor-1-independent regulation of vascular endothelial growth factor by hypoxia in colon cancer. *Cancer Res.* **64**, 1765–1772 (2004).
11. Pierce, J.W. *et al.* Novel inhibitors of cytokine-induced IkappaBalpha phosphorylation and endothelial cell adhesion molecule expression show anti-inflammatory effects *in vivo*. *J. Biol. Chem.* **272**, 21096–21103 (1997).
12. Schreck, R., Rieber, P. & Baeuerle, P.A. Reactive oxygen intermediates as apparently widely used messengers in the activation of the NF-kappa B transcription factor and HIV-1. *EMBO J.* **10**, 2247–2258 (1991).
13. Michiels, C., Minet, E., Mottet, D. & Raes, M. Regulation of gene expression by oxygen: NF-kappaB and HIF-1, two extremes. *Free Radic. Biol. Med.* **33**, 1231–1242 (2002).
14. Chandel, N.S. *et al.* Mitochondrial reactive oxygen species trigger hypoxia-induced transcription. *Proc. Natl. Acad. Sci. USA* **95**, 11715–11720 (1998).
15. Chandel, N.S. *et al.* Reactive oxygen species generated at mitochondrial complex III stabilize hypoxia-inducible factor-1alpha during hypoxia: a mechanism of O2 sensing. *J. Biol. Chem.* **275**, 25130–25138 (2000).
16. Brand, K.A. & Hermfisse, U. Aerobic glycolysis by proliferating cells: a protective strategy against reactive oxygen species. *FASEB J.* **11**, 388–395 (1997).
17. Seagroves, T.N. *et al.* Transcription factor HIF-1 is a necessary mediator of the pasteur effect in mammalian cells. *Mol. Cell. Biol.* **21**, 3436–3444 (2001).
18. Sparmann, A. & Bar-Sagi, D. Ras-induced interleukin-8 expression plays a critical role in tumor growth and angiogenesis. *Cancer Cell* **6**, 447–458 (2004).
19. Shirasawa, S., Furuse, M., Yokoyama, N. & Sasazuki, T. Altered growth of human colon cancer cell lines disrupted at activated Ki-ras. *Science* **260**, 85–88 (1993).
20. Ryan, H.E., Lo, J. & Johnson, R.S. HIF-1 alpha is required for solid tumor formation and embryonic vascularization. *EMBO J.* **17**, 3005–3015 (1998).
21. Beasley, N.J. *et al.* Hypoxia-inducible factors HIF-1alpha and HIF-2alpha in head and neck cancer: relationship to tumor biology and treatment outcome in surgically resected patients. *Cancer Res.* **62**, 2493–2497 (2002).
22. Raval, R.R. *et al.* Contrasting properties of hypoxia-inducible factor 1 (HIF-1) and HIF-2 in von Hippel-Lindau-associated renal cell carcinoma. *Mol. Cell. Biol.* **25**, 5675–5686 (2005).
23. Mack, F.A., Patel, J.H., Biju, M.P., Haase, V.H. & Simon, M.C. Decreased growth of Vhl−/− fibrosarcomas is associated with elevated levels of cyclin kinase inhibitors p21 and p27. *Mol. Cell. Biol.* **25**, 4565–4578 (2005).
24. Koshiji, M. & Huang, L.E. Dynamic balancing of the dual nature of HIF-1alpha for cell survival. *Cell Cycle* **3**, 853–854 (2004).
25. Arenberg, D.A. *et al.* Inhibition of interleukin-8 reduces tumorigenesis of human non-small cell lung cancer in SCID mice. *J. Clin. Invest.* **97**, 2792–2802 (1996).
26. Ofori-Darko, E. *et al.* An OmpA-like protein from *Acinetobacter spp.* stimulates gastrin and interleukin-8 promoters. *Infect. Immun.* **68**, 3657–3666 (2000).
27. Khokhlatchev, A. *et al.* Identification of a novel Ras-regulated proapoptotic pathway. *Curr. Biol.* **12**, 253–265 (2002).
28. Zhang, L., Fogg, D.K. & Waisman, D.M. RNA interference-mediated silencing of the S100A10 gene attenuates plasmin generation and invasiveness of Colo 222 colorectal cancer cells. *J. Biol. Chem.* **279**, 2053–2062 (2004).
29. Behre, G., Smith, L.T. & Tenen, D.G. Use of a promoterless Renilla luciferase vector as an internal control plasmid for transient co-transfection assays of Ras-mediated transcription activation. *Biotechniques* **26**, 24–28 (1999).
30. Mohanty, J.G., Jaffe, J.S., Schulman, E.S. & Raible, D.G. A highly sensitive fluorescent micro-assay of H2O2 release from activated human leukocytes using a dihydroxyphenoxazine derivative. *J. Immunol. Methods* **202**, 133–141 (1997).

CORRIGENDUM: Combating diabetes and obesity in Japan

Y Yazaki & T Kadowaki
Nat. Med. 12, 73–74 (2006)

In **Box 1**, "(BM ≥125)" should read "(BMI ≥25)."

CORRIGENDUM: ATM regulates target switching to escalating doses of radiation in the intestines

H-J Ch'ang, J G Maj, F Paris, H R Xing, J Zhang, J-P Truman, C Cardon-Cardo, A Haimovitz-Friedman, R Kolesnick & Z Fuchs
Nat. Med. 11, 484–490 (2005)

In **Figure 2a**, ceramide levels at 8 and 12 h after 16 Gy should have read 102 ± 10 and 118 ± 10 percent of control, respectively, and s.e.m. values for the remaining points should be multiplied by a factor of 2.6.

CORRIGENDUM: Induction of interleukin-8 preserves the angiogenic response in HIF-1α–deficient colon cancer cells

Y Mizukami, W-S Jo, E-M Duerr, M Gala, J Li, X Zhang, M A Zimmer, O Iliopoulos, L R Zukerberg, Y Kohgo, M P Lynch, B R Rueda & D C Chung
Nat. Med. 11, 992–997 (2005)

In **Figure 3d**, the labels for the cell lines are incorrect. Instead of DLD-1/HIF-wt and DLD-1/HIF-kd, the labels should be Caco2/HIF-wt and Caco2/HIF-kd, respectively.

GASTROENTEROLOGY 2005;128:975–986

Therapeutic Effects of Rectal Administration of Basic Fibroblast Growth Factor on Experimental Murine Colitis

MINORU MATSUURA,* KAZUICHI OKAZAKI,† AKIYOSHI NISHIO,* HIROSHI NAKASE,* HIROYUKI TAMAKI,* KAZUSHIGE UCHIDA,* TOSHIKI NISHI,* MASANORI ASADA,* KIMIO KAWASAKI,* TOSHIRO FUKUI,* HAZUKI YOSHIZAWA,* SHINYA OHASHI,* SATOKO INOUE,* CHIHARU KAWANAMI,* HIROSHI HIAI,§ YASUHIKO TABATA,‖ and TSUTOMU CHIBA*

*Department of Gastroenterology and Endoscopic Medicine, Graduate School of Medicine, §Department of Pathology and Biology of Diseases, and ‖Department of Biomaterials, Institute for Frontier Medical Sciences, Kyoto University, Kyoto; and †Third Department of Internal Medicine, Kansai Medical University, Osaka, Japan

Background & Aims: Basic fibroblast growth factor (bFGF) is a promising therapeutic agent for various diseases. It remains unclear, however, whether bFGF is effective for the treatment of inflammatory bowel disease. The aim of this study was to examine the efficacy of bFGF on 2 experimental murine colitis models and to investigate its molecular mechanisms. *Methods:* We evaluated the effects of human recombinant bFGF (hrbFGF) on mice with dextran sulfate sodium (DSS)-induced colitis and mice with trinitrobenzene sulfonic acid (TNBS)-induced colitis as well as normal mice. Body weight, survival rate, and histologic findings of the colonic tissues were examined. Gene expression of tumor necrosis factor (TNF)-α, cyclooxygenase (COX)-2, transforming growth factor (TGF)-β, mucin 2 (MUC2), intestinal trefoil factor (ITF), and vascular endothelial growth factor (VEGF) in the colonic tissues was determined. The proliferation activity of hrbFGF on the colonic epithelium was evaluated by immunohistochemistry. *Results:* Rectal administration of hrbFGF ameliorated DSS-induced colitis in a dose-dependent manner. Gene expression of TNF-α was significantly reduced in the colonic tissues of mice with DSS-induced colitis treated with hrbFGF, whereas MUC2 and ITF messenger RNA expression was up-regulated. Rectal administration of hrbFGF significantly improved the survival rate of mice with TNBS-induced colitis and partially ameliorated colitis. hrbFGF significantly increased the number of Ki-67–positive cells in the colonic epithelium of normal mice, and up-regulated the gene expression of COX-2, TGF-β, MUC2, ITF, and VEGF in the colonic tissues. *Conclusions:* Rectal administration of bFGF might be a promising option for the treatment of inflammatory bowel disease.

Although the cause of inflammatory bowel disease (IBD) remains unclear, it has been suggested that immunologic abnormality has a key role in the pathogenesis of human IBD.[1] Indeed, several immune-regulatory agents, such as corticosteroids, 5-aminosalicylates, immunosuppressants, and anti–tumor necrosis factor (TNF)-α monoclonal antibody, have mainly been used for the treatment of human IBD to control the dysregulated immune response. There are some patients with IBD, however, who are refractory even to the combined use of these agents. In the pathogenesis of IBD, recent clinical and experimental studies have shown that impaired intestinal barrier function permits penetration of toxic and immunogenic factors, which lead to the induction and perpetuation of intestinal inflammation.[2] Therefore, enhancement of intestinal barrier function, which could reduce inflammation caused by decreased uptake of luminal antigens and bacteria, may also provide an effective approach as a novel therapeutic strategy for IBD.

Growth factors have various biologic actions, such as enhancement of cell proliferation, modulation of cell differentiation, and acceleration of cell migration, angiogenesis, and extracellular matrix remodeling.[3,4] A number of growth factors are expressed in the gastrointestinal tract, including members of the epidermal growth factor (EGF) family, the transforming growth factor (TGF)-β family, the fibroblast growth factor (FGF) family, the insulin-like growth factor family, and so on.[5] These growth factors have essential roles in regulating diverse epithelial cell functions, not only to preserve normal homeostasis and the integrity of the intestinal mucosa

Abbreviations used in this paper: bFGF, basic fibroblast growth factor; COX, cyclooxygenase; DSS, dextran sulfate sodium; EGF, epidermal growth factor; FGF, fibroblast growth factor; hrbFGF, human recombinant basic fibroblast growth factor; IL, interleukin; ITF, intestinal trefoil factor; KGF, keratinocyte growth factor; MLN, mesenteric lymph nodes; MUC2, mucin 2; PCR, polymerase chain reaction; PPAR, peroxisome proliferator-activated receptor; TGF, transforming growth factor; TNBS, trinitrobenzene sulfonic acid; TNF, tumor necrosis factor; VEGF, vascular endothelial growth factor.

0016-5085/05/$30.00
doi:10.1053/j.gastro.2005.01.006

but also to repair mucosal injury.[5] Therefore, they might serve as an alternative therapy for patients with IBD. Indeed, 2 clinical trials using growth factors were recently performed in patients with active ulcerative colitis. A phase 2 study of keratinocyte growth factor (KGF)-2 in patients with active ulcerative colitis showed that intravenous administration of KGF-2 at a dose of 1–50 μg/kg was not effective for inducing remission.[6] However, a placebo-controlled trial of EGF enemas in patients with active left-sided ulcerative colitis or proctitis showed that the remission rate in the EGF-treated group was significantly higher than in the group receiving placebo.[7] Thus, it has not yet been determined whether growth factors are useful for the treatment of human IBD.

Basic fibroblast growth factor (bFGF, also known as FGF-2) was initially regarded as a potent angiogenic factor because it induces endothelial cell proliferation, migration, and smooth muscle cell proliferation.[8,9] Previous studies have shown that administration of bFGF improved myocardial infarction with developing collateral vessels in experimental models of ischemic heart disease.[10,11] Moreover, based on its pleiotropic function, which has important roles in the differentiation and/or function of the skin, the eye, and the nervous system,[12] bFGF has already been administered as a potential therapeutic agent in various experimental models.[13–20] Those experimental studies showed that bFGF stimulated wound repair in various organs. Additionally, FGF-2 knockout mice show reduced reepithelialization and collagen deposition after skin injury.[21] Those data strongly suggested that bFGF plays a pivotal role in the repair process of wound injury. In the gastrointestinal tract, bFGF enhances epithelial cell proliferation and restitution as well as stem cell survival after radiation injury to the intestine.[22,23] These data suggest that bFGF might be a promising agent in the treatment of mucosal injury in human IBD.

Therefore, in the present study, we examined the efficacy of rectal administration of human recombinant bFGF (hrbFGF) on 2 experimental murine colitis models (ie, dextran sulfate sodium [DSS]-induced colitis and trinitrobenzene sulfonic acid [TNBS]-induced colitis) and investigated the molecular mechanisms of actions of hrbFGF on healing intestinal mucosal injury.

Materials and Methods

Animals

Female C57BL/6 mice (8–10 weeks old; Japan SLC, Inc, Shizuoka, Japan) and female SJL/J mice (10–11 weeks old; Charles River Japan, Inc, Kanagawa, Japan) were used for the experiments. They were fed with standard laboratory chow and tap water ad libitum. All mice were housed in specific pathogen–free conditions in the animal facility of Kyoto University. The studies were approved by the animal protection committee of our institution.

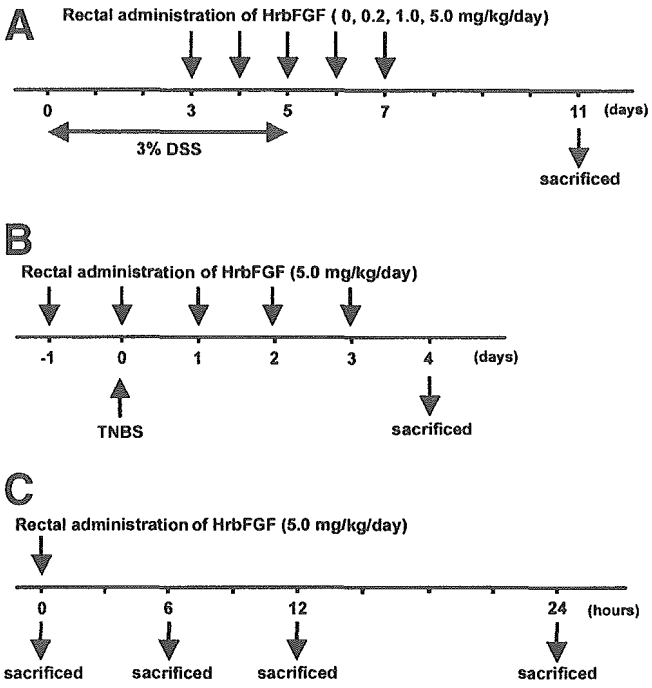

Figure 1. Experimental protocols of the study. (*A*) Study with DSS-induced colitis mice; (*B*) study with TNBS-induced colitis mice; and (*C*) study with normal mice.

Effects of hrbFGF on Experimental Murine Colitis

DSS-induced colitis model. *Induction of colitis.* To induce colitis, C57BL/6 mice were given 3% DSS (mol wt, 36–50 kilodaltons; ICN Biomedicals, Inc, Aurora, OH) in their drinking water for 5 days (from day 0 to 4). On day 5, they were switched to regular drinking water. Normal control mice received regular drinking water throughout the experiment.

Treatments. Forty mice with DSS-induced colitis were divided into 4 groups (n = 10 in each group) and treated with rectal administration of hrbFGF as follows: 0 (no medication), 0.2, 1.0, or 5.0 mg · kg^{-1} · day^{-1}. Another 10 mice were used as normal controls without DSS treatment. hrbFGF was a generous gift from Kaken Pharmaceutical Co Ltd (Tokyo, Japan). hrbFGF was diluted in 150 μL phosphate-buffered saline (PBS) and rectally administered once a day for 5 consecutive days starting from 3 days after the initiation of DSS treatment (Figure 1*A*). After each rectal administration of hrbFGF, mice were kept in an inverted position for 30 seconds. Both normal and nontreated colitis-induced mice received PBS as a vehicle solution via the rectum. Body weight was measured daily throughout the experiment. All mice were monitored for 6 additional days after DSS treatment and killed on

day 11 by cervical dislocation (Figure 1*A*). The colonic tissue was removed from each mouse and examined as described in the following text.

Macroscopic appearance. At necropsy, the length from the ileocecal junction to the anal verge was measured as the colonic length.

Microscopic assessment of colonic damage. The distal third of the colon was evaluated because this segment is most severely affected in DSS-induced colitis.[24] The entire colon was removed, opened longitudinally, and washed with PBS. The distal third of the colon was dissected, and then the longitudinal section (1.5 cm from the anal verge) was prepared. The sections were fixed in 3.6% formaldehyde, stained with H&E, and histologically analyzed in a blind manner. Histologic damage was quantified by the histologic scoring system described by Williams et al.[25] In brief, the sections were graded as to inflammation severity, inflammation extent, and crypt damage. The grading index for inflammation severity was as follows: 0, none; 1, mild; 2, moderate; 3, severe. The grading index for inflammation extent was as follows: 0, none; 1, mucosa; 2, mucosa and submucosa; 3, transmural. The grading index for crypt damage was as follows: 0, none; 1, basal one third damaged; 2, basal two thirds damaged; 3, crypts lost but surface epithelium present; 4, crypts and surface epithelium lost. Each of these grades was also scored as to the percent involvement (0, 0%; 1, 1%–25%; 2, 26%–50%; 3, 51%–75%; 4, 76%–100%). Each subscore (inflammation severity score, inflammation extent score, and crypt damage score) was the product of the grade multiplied by the percent involvement. The total colitis score was the sum of the 3 subscores.

Quantitative analysis of gene expressions of proinflammatory cytokine and mucosal repair-related molecules. Samples of colonic tissue for messenger RNA (mRNA) isolation were removed from the distal third of the colon. Total RNA was extracted using the guanidium isothiocyanate-phenol-chloroform method. RNA (1 μg) was reverse transcribed with MultiScribe reverse transcriptase (Applied Biosystems, Foster City, CA), and the resulting complementary DNAs (50 ng/reaction mixture) were analyzed for TNF-α, cyclooxygenase (COX)-2, TGF-β, mucin 2 (MUC2), intestinal trefoil factor (ITF), and vascular endothelial growth factor (VEGF) mRNA expression by real-time polymerase chain reaction (PCR) using an ABI Prism 7700 sequence detection system (Applied Biosystems). The reaction mixtures were incubated for 2 minutes at 50°C, denatured for 10 minutes at 95°C, and subjected to 45 amplification cycles consisting of annealing and extension at 60°C for 1 minute followed by denaturation at 95°C for 15 seconds. The primers and probes used for this experiment were obtained from Applied Biosystems. Quantification of mRNA was performed using the $\Delta\Delta C_T$ method.[26,27] Gene expression levels of target molecules were normalized using the housekeeping gene, glyceraldehyde-3-phosphate dehydrogenase, amplified using TaqMan rodent glyceraldehyde-3-phosphate dehydrogenase control reagents (Applied Biosystems).

Flow cytometry analysis for activated T cells in mesenteric lymph nodes. To investigate the effect of hrbFGF on T cells in vivo, we analyzed the number of activated T cells in mesenteric lymph nodes (MLN) by flow cytometry analysis. On day 8, mice with DSS-induced colitis with or without hrbFGF treatment (5.0 mg · kg^{-1} · day^{-1}) were killed, and the MLN were removed (n = 3 in each group; Figure 1*A*). Isolated MLN were gently teased apart using an aseptic 27-gauge needle, and single cells were suspended in RPMI 1640 medium (Invitrogen Corp, Carlsbad, CA) supplemented with 5% heat-inactivated fetal calf serum, 50 μg/mL gentamicin, and 50 μmol/L 2-mercaptoethanol. Cells (1×10^6) were preincubated with normal mouse serum for 30 minutes on ice and then stained with both phycoerythrin-conjugated monoclonal antibody against CD4 (BD PharMingen, San Diego, CA) and fluorescein isothiocyanate–conjugated monoclonal antibody against CD69 (BD PharMingen). Cells were washed with PBS and analyzed using a flow cytometer and System II software (EPICS XL; Beckman Coulter, Inc, Fullerton, CA).

TNBS-induced colitis model. *Induction of colitis.* TNBS colitis was induced in SJL/J mice by using a modification of the method described by Neurath et al.[28] In brief, 5.0 mg of the hapten reagent TNBS (Sigma Chemical Co, St. Louis, MO) in 50% ethanol was slowly administered into the lumen of the colon (about 4.0 cm from the anal verge) using the catheter fitted onto a 1-mL syringe under diethyl ether anesthesia. Another 5 mice received 50% ethanol alone as vehicle control using the same technique. The total injection volume was 200 μL in both groups. Mice were then kept in an inverted position for 30 seconds. Mice were killed at 4 days after administration of TNBS (Figure 1*B*).

Treatments. Mice with TNBS-induced colitis (n = 12) were treated with rectal administration of hrbFGF (5.0 mg · kg^{-1} · day^{-1}) for 5 consecutive days, beginning on the day before the initiation of TNBS administration (ie, day −1) (Figure 1*B*). Another 16 mice with TNBS-induced colitis received PBS via rectum as a nontreated group (Figure 1*B*).

Evaluations. For assessment of the efficacy of hrbFGF on TNBS-induced colitis, we evaluated the survival rate and histologic findings of colonic tissues. For histologic examination, 2 distal colonic regions spaced approximately 1 cm apart were collected into 3.6% formaldehyde, processed for paraffin embedding, sectioned, and stained with H&E. The degree of colonic inflammation and cryptal regeneration was graded in a blind manner using a histologic scoring system described by Elson et al with some modifications.[29] Briefly, the sections were graded as to inflammation severity, inflammation extent, and regeneration. The grading index for inflammation severity was as follows: 0, none; 1, mild; 2, moderate; 3, severe. The grading index for inflammation extent was as follows: 0, none; 1, mucosa; 2, mucosa and submucosa; 3, transmural. The grading index for regeneration was as follows: 0, complete cryptal regeneration; 1, broad, multifocal cryptal regeneration; 2, partial cryptal regeneration; 3, focal migration and mitotic figures of colonic epithelium or scattered cryptal regeneration; 4, none. Each subscore of 2 histologic segments was averaged.

Table 1. Primer Pairs for Semiquantitative PCR

Target gene	Primer sequences	Major product size (*base pairs*)
COX-2	Forward: 5′-gtctgatgatgtatgccaccatctg-3′ Reverse: 5′-gcatctggacgaggtttttc-3′	658
TGF-β	Forward: 5′-tggaccgcaacaacgccatctatgagaaaacc-3′ Reverse: 5′-tggagctgaagcaatagttggtatccagggct-3′	525
MUC2	Forward: 5′-cgacaccagggctttcgcttaat-3′ Reverse: 5′-cacttccaccctcccggcaaac-3′	501
ITF	Forward: 5′-tctggctaatgctgttggtgg-3′ Reverse: 5′-atcagccttgtgttggctgtg-3′	388
VEGF	Forward: 5′-cacgacagaaggagagcagaagtc-3′ Reverse: 5′-tcaacggtgacgatgatggc-3′	594
IL-10	Forward: 5′-atgcaggactttaagggttacttgggtt-3′ Reverse: 5′-atttcggagagaggtacaaacgaggttt-3′	455
PPAR-γ	Forward: 5′-cctctccgtgatggaagacc-3′ Reverse: 5′-gcattgtgagacatccccac-3′	404
β-actin	Forward: 5′-gtgggccgctctaggcaccaa-3′ Reverse: 5′-ctctttgatgtcacgcacgatttc-3′	540

Inflammation score is the sum of inflammation severity and inflammation extent, and thus a score of 8 indicates most severe colonic inflammation. Maximum score of regeneration is 4, indicating no mucosal regeneration, while minimum score is 0, indicating complete mucosal regeneration.

Effects of hrbFGF on Normal Colonic Mucosa

Proliferating effects of hrbFGF on intestinal epithelial cells. To investigate the proliferation activity of hrbFGF on colonic epithelium in vivo, we performed immunohistochemical staining against the Ki-67 antigen. hrbFGF (5.0 mg/kg) was rectally administered to 8-week-old female C57BL/6 mice (n = 3) 24 hours before necropsy. Control mice (n = 3) received PBS alone via the rectum. Paraffin-embedded sections (4 μm thick) were prepared, deparaffinized, and reacted with 0.3% H_2O_2 in methanol for 30 minutes to inhibit endogenous peroxidase activity. The sections were placed in 0.01 mol/L citrate buffer (pH 6.0) and pretreated with microwave heating for antigen retrieval. After blocking with 3% bovine serum albumin in PBS, the sections were incubated with anti-mouse Ki-67 monoclonal antibody (Dako Cytomation, Copenhagen, Denmark) diluted 1:200 in PBS with 1% bovine serum albumin overnight at 4°C. After washing with PBS, the sections were incubated with biotinylated anti-rat immunoglobulin G antibody for 30 minutes and then reacted with a peroxidase-linked avidin-biotin complex (Vector Laboratories, Burlingame, CA) diluted 1:100 in PBS with 1% bovine serum albumin for 30 minutes. Localization of the Ki-67 antigen was visualized by incubation with 3,3′-diaminobenzidine tetrahydrochloride in 0.05% H_2O_2 for 1 minute. Hematoxylin was used for nuclear counterstaining. Longitudinally sectioned crypts, for which the entire length was visible, were selected in each sample. The number of Ki-67–positive cells in 500 epithelial cells was counted under a microscope at 200× magnification. The Ki-67 labeling index was defined as the percentage of Ki-67–positive cells among the counted epithelial cells.

Effects of hrbFGF on the gene expression of mucosal repair-related or anti-inflammatory molecules. Next, we examined the effects of hrbFGF on the gene expression of various molecules involved in the mucosal repair process, such as COX-2, TGF-β, MUC2, ITF, and VEGF by semiquantitative PCR. In addition, we also investigated whether administration of hrbFGF could up-regulate the gene expression of anti-inflammatory molecules, such as interleukin (IL)-10 and peroxisome proliferator-activated receptor (PPAR)-γ. To exclude the influence of inflammatory conditions on those gene expressions, hrbFGF (5.0 mg/kg) was given rectally as a single administration to normal mice. The colonic tissues were collected at 0, 6, 12, and 24 hours after administration of hrbFGF (n = 3 in each group; Figure 1*C*). Total tissue RNA was prepared using the same method as described previously. RNA was reverse transcribed using 5 μg of total RNA according to the manufacturer's instructions. PCR was performed in a volume of 20 μL containing 1 μL of complementary DNA, 0.5 mmol/L of each primer, and a solution of 1 U of *Taq* DNA polymerase using the GeneAmp PCR System 9600 (Perkin-Elmer Corp, Norwalk, CT). The PCR primer sequences used are shown in Table 1. PCR products were separated on 1% agarose gels containing ethidium bromide. After gel electrophoresis, band densities were measured using an autoanalyzing system (Fotodyne, FOTO/Analyst, and Archiver Eclipse; Advanced American Biotechnology, Fullerton, CA). The COX-2, TGF-β, MUC2, ITF, VEGF, IL-10, and PPAR-γ signals were standardized against the β-actin signal for each sample, and results were expressed as the ratio of each molecule to β-actin.

Effects of hrbFGF on TGF-β Production in Colon-26 and NIH3T3 Cells in Vitro

The murine colonic epithelial cell line Colon-26 and the murine fibroblast cell line NIH3T3 were used for the experiments. Colon-26 cells were maintained with RPMI medium 1640 (Invitrogen Corp) supplemented with 10% heat-inactivated fetal calf serum and antibiotics (100 U/mL peni-

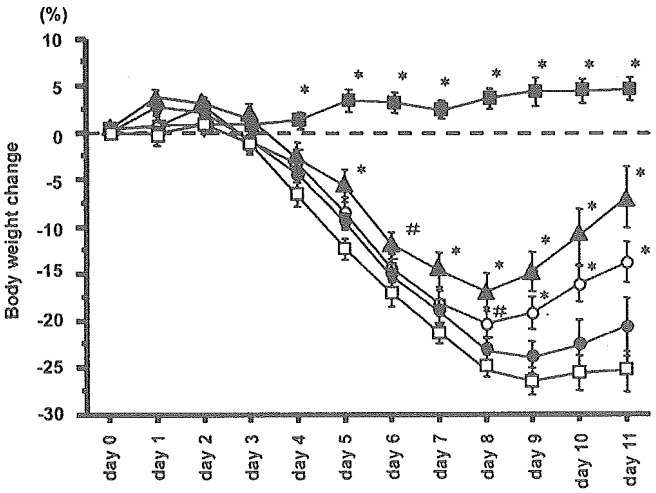

Figure 2. Therapeutic effects of hrbFGF on body weight changes in mice with DSS-induced colitis. Serial changes of body weight were measured daily throughout the experiment. Data are expressed as the mean percent change from starting body weight. Results represent means ± SD (n = 10 in each group). *Open squares*, nontreated mice with DSS-induced colitis; *closed circles*, mice with DSS-induced colitis treated with 0.2 mg/kg of hrbFGF; *open circles*, mice with DSS-induced colitis treated with 1.0 mg/kg of hrbFGF; *closed triangles*, mice with DSS-induced colitis treated with 5.0 mg/kg of hrbFGF; *closed squares*, normal mice. $^{*}P < .01$ and $^{\#}P < .05$ compared with nontreated mice with DSS-induced colitis.

cillin and 100 μg/mL streptomycin). NIH3T3 cells were cultured with Dulbecco's modified Eagle medium (ICN Biomedicals, Inc) supplemented with 10% heat-inactivated fetal calf serum and antibiotics (as previously described). Cells were seeded into 24-well plates (1×10^5 cells/well) and grown to confluence in basal medium. After that, cells were incubated for 24 hours in serum-free basal medium supplemented with 1% Nutridoma-SP (Roche Diagnostics Corp, Indianapolis, IN) and then were stimulated with hrbFGF (100 ng/mL) plus heparin (10 μg/mL). The conditioned media were collected at the indicated points and assessed for the amount of total TGF-β1 protein by enzyme-linked immunosorbent assay using a TGF-β1 E_{max} ImmunoAssay System (Promega Corp, Madison, WI) according to the manufacturer's instructions.

Statistical Analysis

Student *t* test and the Mann–Whitney *U* test were used where appropriate for statistical analysis. Cumulative survival rate was calculated by the Kaplan–Meier method, and survival curves were compared by log-rank test. The data are expressed as mean ± SD. A 2-tailed *P* value of <.05 was considered statistically significant.

Results

Effects of hrbFGF on DSS-Induced Colitis

Body weight change. In the nontreated mice with DSS-induced colitis, body weight gradually decreased and did not recover at the end of the experiment. On the other hand, the body weight in mice with DSS-induced colitis treated with 1.0 or 5.0 mg/kg of hrbFGF significantly recovered in a dose-dependent manner compared with the nontreated mice with DSS-induced colitis (Figure 2).

Colonic length. The colonic length in the nontreated mice with DSS-induced colitis was significantly shorter than in normal mice. The colonic length in mice with DSS-induced colitis treated with 5.0 mg/kg of hrbFGF was significantly greater than in the nontreated mice with DSS-induced colitis ($P < .01$). However, there were no significant differences in colonic length between the nontreated mice with DSS-induced colitis and the groups treated with 0.2 or 1.0 mg/kg of hrbFGF (Figure 3).

Representative histologic findings of the colonic tissues. In both the nontreated and hrbFGF-treated (5.0 mg/kg) mice with DSS-induced colitis, the histologic findings revealed epithelial destruction, remarkable infiltration of inflammatory cells, and submucosal edema (Figure 4*B* and *C*). In contrast, in mice with DSS-induced colitis treated with 1.0 mg/kg of hrbFGF, crypt regeneration and restoration of colonic mucosa were observed, although there was a limited amount of cellular infiltration and edema in the lamina propria and submucosa (Figure 4*D*). Moreover, histologic findings of mice with DSS-induced colitis treated with 5.0 mg/kg of hrbFGF were essentially normal (except in 3 mice), al-

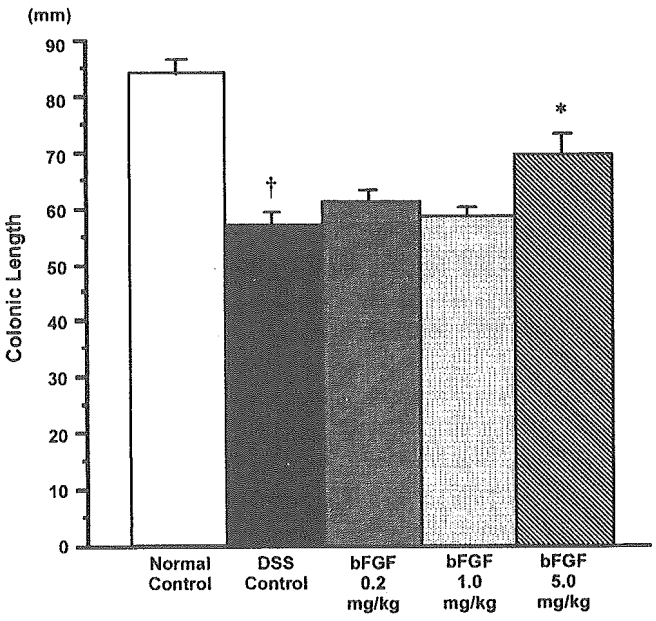

Figure 3. Effects of rectal administration of hrbFGF on colonic length in mice with DSS-induced colitis. Colonic length was measured from the ileocecal junction to the anal verge at necropsy (on day 11). Data are expressed as means ± SD (n = 10 in each group). $^{*}P < .01$ compared with nontreated mice with DSS-induced colitis. $^{\dagger}P < .01$ compared with normal mice.

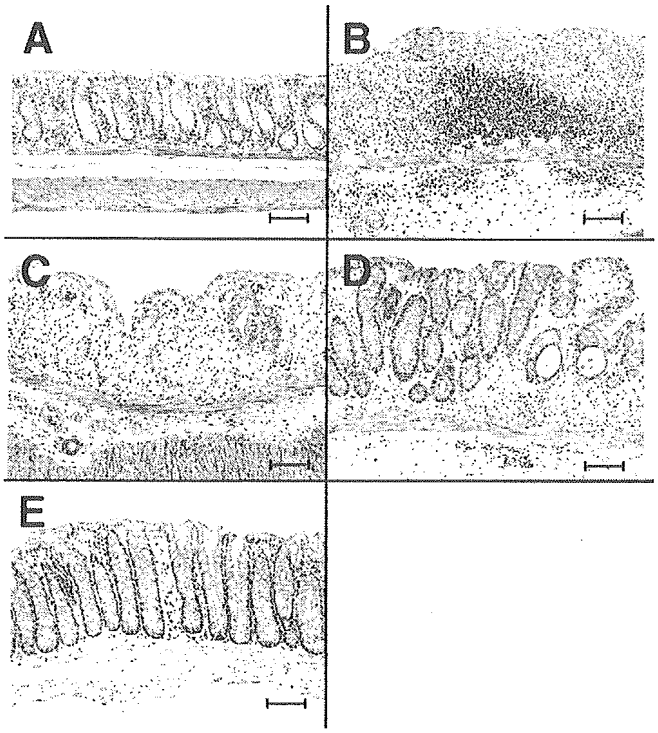

Figure 4. Representative histologic findings in mice with DSS-induced colitis treated with hrbFGF. Sections of the distal colon were collected at necropsy (on day 11) and stained with H&E. (*A*) Normal mice, (*B*) nontreated mice with DSS-induced colitis, (*C*) mice with DSS-induced colitis treated with 0.2 mg/kg of hrbFGF, (*D*) mice with DSS-induced colitis treated with 1.0 mg/kg of hrbFGF, and (*E*) mice with DSS-induced colitis treated with 5.0 mg/kg of hrbFGF. *Bars* = 100 μm. (Original magnification 200×.)

though there was slight infiltration of mononuclear cells and neutrophils (Figure 4*E*).

Histologic evaluation. Rectal administration of 1.0 or 5.0 mg/kg of hrbFGF dose-dependently and significantly reduced both the subscores and the total colitis scores in mice with DSS-induced colitis compared with the nontreated mice with DSS-induced colitis (Figure 5). On the other hand, administration of 0.2 mg/kg of hrbFGF significantly improved only the inflammatory severity score (Figure 5).

Gene expression of proinflammatory cytokines and mucosal repair-related molecules in mice with DSS-induced colitis with and without hrbFGF treatment. The gene expression of TNF-α and COX-2 in the nontreated mice with DSS-induced colitis was significantly higher than in normal mice. mRNA expression of TNF-α and COX-2 in mice with DSS-induced colitis treated with 5.0 mg/kg of hrbFGF was significantly lower than in the nontreated mice with DSS-induced colitis (Figure 6). There were no significant differences in TNF-α and COX-2 expression between the nontreated and hrbFGF-treated (0.2 or 1.0 mg/kg) mice with DSS-induced colitis (Figure 6). Similar trends were observed in TGF-β and VEGF mRNA expression in mice with DSS-induced colitis treated with hrbFGF, although there was no statistical significance (Figure 6). On the other hand, gene expression of MUC2 and ITF in the nontreated mice with DSS-induced colitis was significantly lower than in normal mice. However, treatment with 5.0 mg/kg of hrbFGF significantly increased both MUC2 and ITF mRNA expression as compared with the nontreated mice with DSS-induced colitis and was even higher than in normal mice, although there were no significant differences (Figure 6).

Expression of CD69 on $CD4^+$ T cells from MLN. There were no significant differences in the number of $CD4^+$ T cells from the MLN between mice with DSS-induced colitis treated with and without hrbFGF ($5.22 \pm 0.59 \times 10^6$ vs $4.81 \pm 0.49 \times 10^6$; $P = .248$). In addition, similar results were observed in the number of $CD4^+CD69^+$ T cells from MLN ($10.65 \pm 0.58 \times 10^5$ vs $9.78 \pm 0.11 \times 10^5$; $P = .564$).

Effects of hrbFGF on TNBS-Induced Colitis

Cumulative survival rate. The overall survival rate of mice with TNBS-induced colitis treated with hrbFGF (5.0 mg/kg) was significantly higher than that of the nontreated mice with TNBS-induced colitis (91.7% vs 56.3%; $P = .0421$; Figure 7*A*).

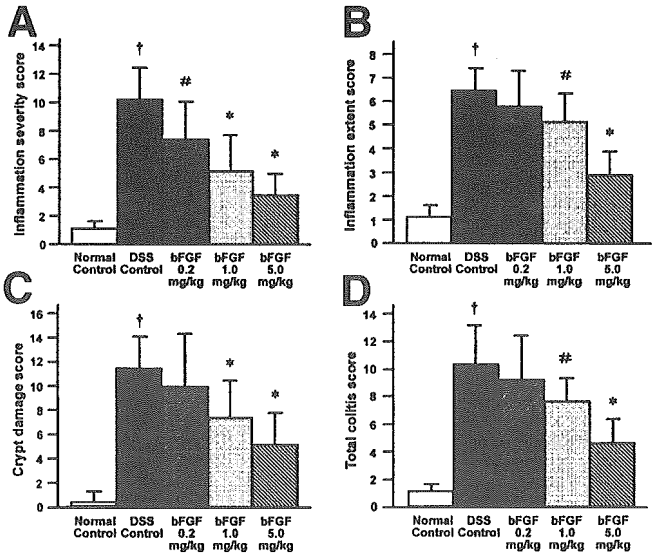

Figure 5. Histologic scores of colonic tissues in mice with DSS-induced colitis treated with hrbFGF. Each subscore was the product of the grade multiplied by the percent involvement. The total colitis score is the sum of the 3 subscores (inflammation severity, inflammation extent, and crypt damage). (*A*) Inflammation severity score, (*B*) inflammatory extent score, (*C*) crypt damage score, and (*D*) total colitis score. Data are expressed as means ± SD (n = 10 in each group). $^*P < .01$ and $^\#P < .05$ compared with nontreated mice with DSS-induced colitis. $^\dagger P < .01$ compared with normal mice.

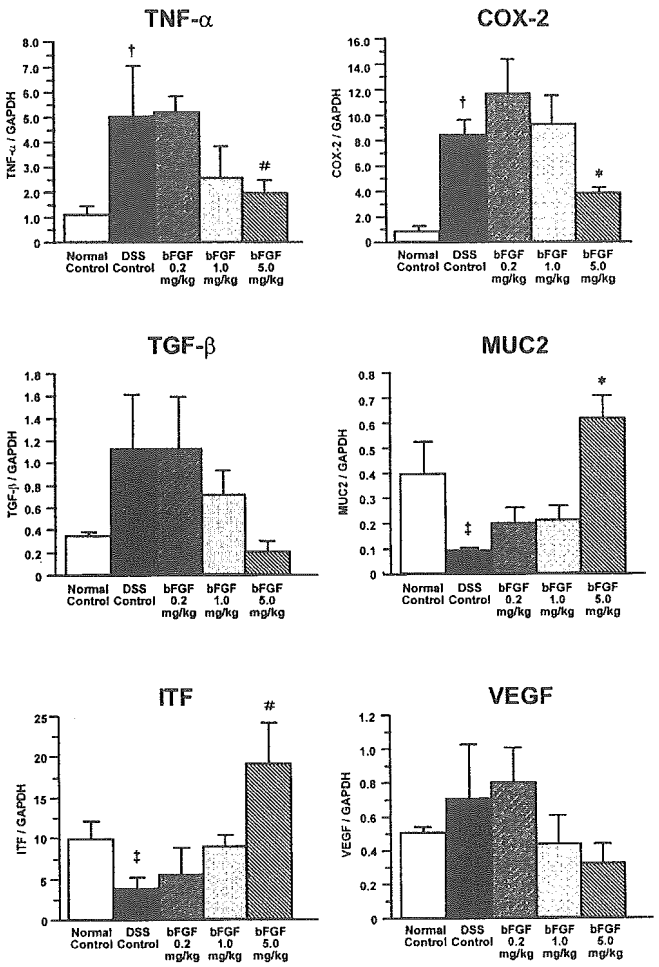

Figure 6. Effects of rectal administration of hrbFGF on the transcript levels of TNF-α, COX-2, TGF-β, MUC2, ITF, and VEGF in the colonic tissues of mice with DSS-induced colitis. The gene expression of each target molecule was determined by real-time PCR and was standardized against glyceraldehyde-3-phosphate dehydrogenase. Data are expressed as means ± SD (n = 5 in each group). $^{*}P < .01$ and $^{\#}P < .05$ compared with nontreated mice with DSS-induced colitis. $^{\dagger}P < .01$ and $^{\ddagger}P < .05$ compared with normal mice.

Representative histologic findings of the colonic tissues. In the nontreated mice with TNBS-induced colitis, the histologic analysis showed lymphocytic infiltrates, ulcerations, loss of cryptal cells, and thickening of the colonic wall. In contrast, in mice with TNBS-induced colitis treated with hrbFGF (5.0 mg/kg), reepithelialization and cryptal regeneration of colonic mucosa were partially observed, although lymphocytic infiltrates still remained (Figure 7*B*).

Histologic evaluation. Rectal administration of hrbFGF (5.0 mg/kg) did not significantly reduce inflammation score in the hrbFGF-treated group compared with the nontreated group (Figure 7*C*). On the contrary, regeneration score in the group treated with hrbFGF tended to be lower than in the nontreated group, although there was no significant difference (Figure 7*C*).

Effects of hrbFGF on Normal Colonic Mucosa

Immunohistochemical staining with anti-Ki-67 monoclonal antibody. In control mice, Ki-67–positive cells were mainly located in the lower third of the crypts (Figure 8*A*, left panel). On the other hand, in mice treated with hrbFGF, Ki-67–positive cells were observed in the lower to middle third of the crypts (Figure 8*A*, right panel). The Ki-67 labeling index in mice treated with hrbFGF was significantly higher than in control mice (Figure 8*B*).

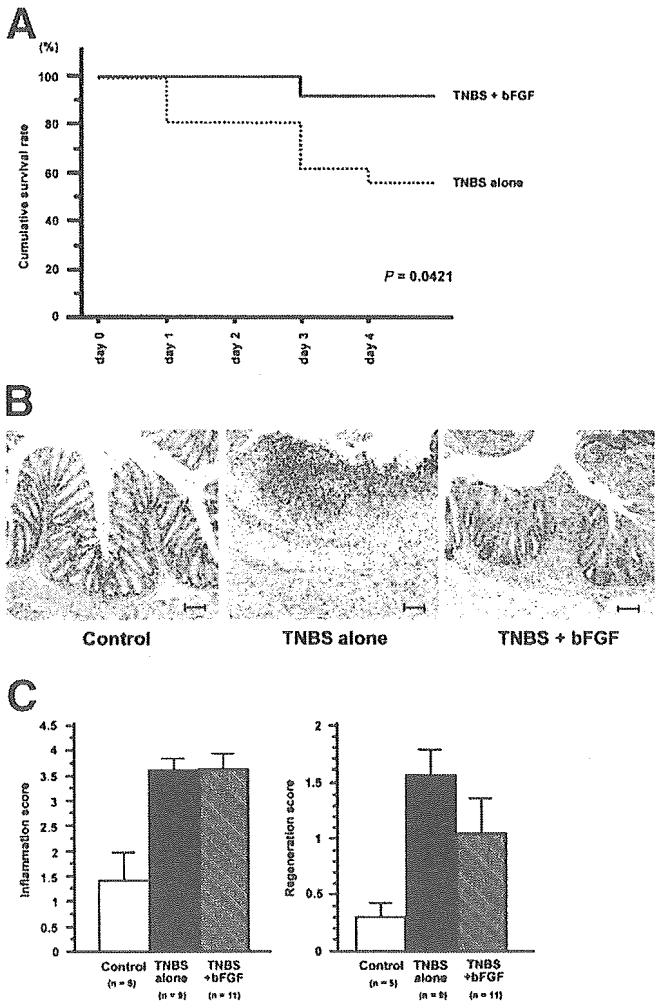

Figure 7. Effects of rectal administration of hrbFGF on murine TNBS-induced colitis. (*A*) Cumulative survival curves in mice with TNBS-induced colitis. *Solid line*, mice with TNBS-induced colitis treated with 5.0 mg/kg of hrbFGF; *dotted line*, nontreated mice with TNBS-induced colitis. (*B*) Representative histologic findings in mice with TNBS-induced colitis. Control, control mice receiving 50% ethanol alone; TNBS alone, nontreated mice with TNBS-induced colitis; TNBS + bFGF, mice with TNBS-induced colitis treated with 5.0 mg/kg of hrbFGF. *Bars* = 100 μm. (Original magnification 100×.) (*C*) Histologic scores (inflammation score and regeneration score) of colonic tissues in mice with TNBS-induced colitis treated with hrbFGF. Inflammation score is the sum of inflammatory severity and inflammatory extent. Data are expressed as means ± SD.

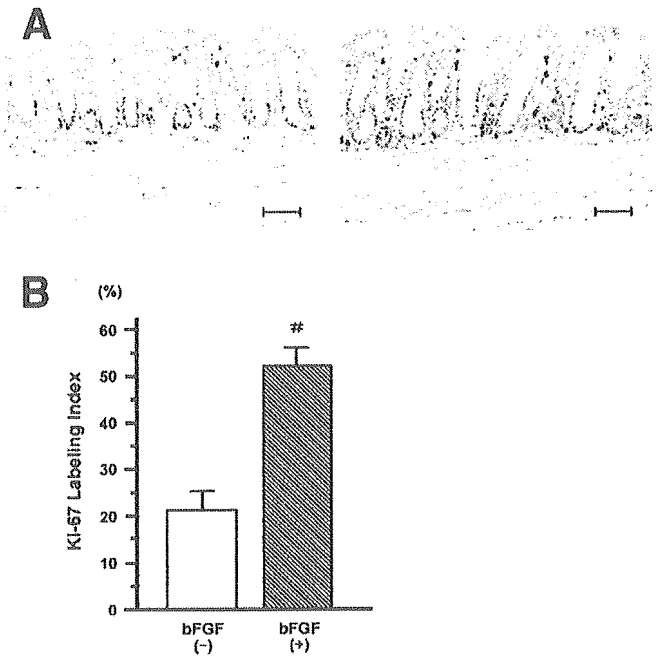

Figure 8. Immunohistochemistry of colonic tissues of normal mice using the anti–Ki-67 monoclonal antibody. (*A*) Representative histologic findings of immunohistochemical staining with anti–Ki-67 monoclonal antibody. *Left panel*, nontreated mice; *right panel*, hrbFGF-treated (5.0 mg/kg) mice. *Bars* = 100 μm. (Original magnification 200×.) (*B*) The Ki-67 labeling index. The Ki-67 labeling index was defined as the percentage of Ki-67–positive cells in the counted crypts. Five hundred nuclei in each sample were counted. Data are expressed as means ± SD (n = 3 in each group). $^{\#}P < .05$ compared with the control group.

Semiquantitative analysis of gene expression of mucosal repair-related and anti-inflammatory molecules. The gene expression of COX-2, TGF-β, ITF, and VEGF in the colonic tissues of normal mice treated with hrbFGF was significantly higher compared with nontreated normal mice (Figure 9). MUC2 mRNA expression in the colonic tissues tended to be up-regulated by treatment with hrbFGF, although there was no significant difference (Figure 9). Maximal up-regulation occurred at 6 hours (ITF), 12 hours (TGF-β, VEGF), or 24 hours (COX-2, MUC2) after hrbFGF administration. On the other hand, IL-10 and PPAR-γ mRNA expression in the colonic tissues of normal mice treated with hrbFGF was not significantly up-regulated compared with nontreated normal mice (data not shown).

Effects of hrbFGF on the Production of TGF-β in Both Epithelial and Fibroblast Cell Lines

To assess the effect of hrbFGF on TGF-β production in vitro, we measured the concentration of TGF-β in the culture media of Colon-26 or NIH3T3 cells after 24 hours of incubation with hrbFGF. In both cell lines, TGF-β production in hrbFGF-stimulated cells was significantly higher than that in nonstimulated cells (Figure 10).

Discussion

For the past 10 years, several growth factors, such as EGF, FGF, insulin-like growth factor, and hepatocyte growth factor, have been tested as potent therapeutic agents in a variety of experimental models of human IBD.[30–36] Among them, a great deal of attention has been paid to the FGF family, especially KGF-1 and KGF-2, because several clinical and experimental studies showed that they are also effective for the treatment of epithelial damage in other tissues, such as skin and oral mucosa.[37–40] Indeed, a clinical trial of KGF-2 has recently been performed for the treatment of active ulcerative colitis.[6] bFGF is also a member of the FGF family and has been shown to be effective for improving epithelial damage of several organs in animal models.[13,15–18] Based on those experimental data, human recombinant

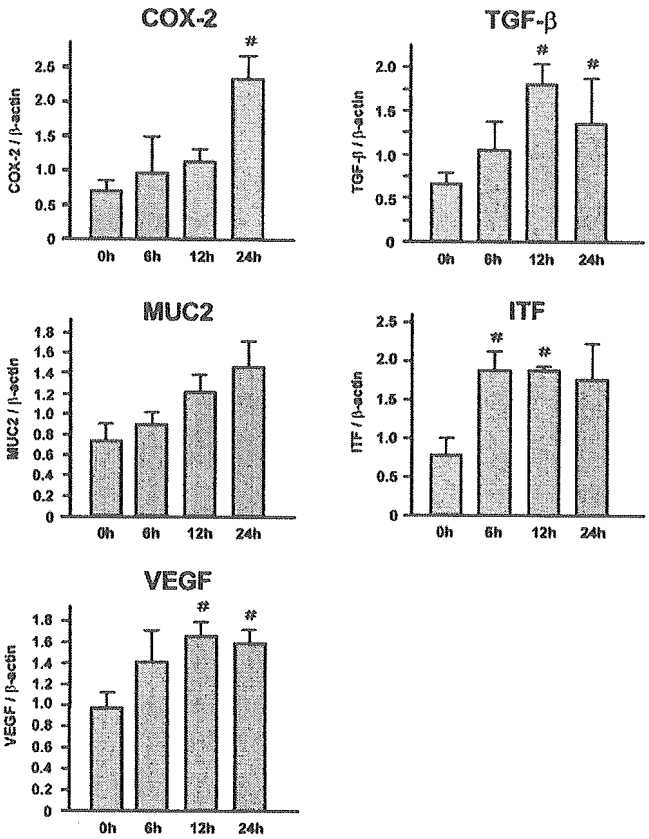

Figure 9. Effects of hrbFGF on the time-course changes of the gene expression of mucosal repair-related molecules in the colonic tissues of normal mice. The expression of each molecule RNA transcript at the indicated time periods was determined by semiquantitative reverse-transcription PCR. The results are expressed as relative ratio of each molecule to β-actin. Data are shown as means ± SD (n = 3 in each group). $^{\#}P < .05$ compared with the control group (0 hours).

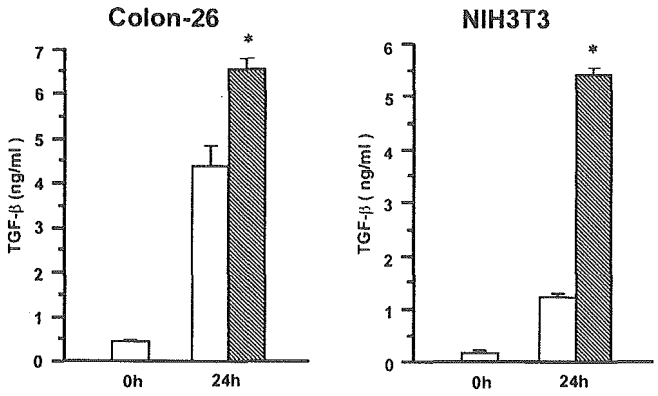

Figure 10. Effects of hrbFGF on TGF-β protein production by Colon-26 and NIH3T3 cells. Both cells were cultured for 24 hours with or without hrbFGF (100 ng/mL). The concentration of TGF-β protein was determined by enzyme-linked immunosorbent assay. *Open columns*, nonstimulated cells; *hatched columns*, hrbFGF-stimulated cells. Data are expressed as means ± SD (n = 4 in each group). $*P < .01$ compared with the conditioned media without hrbFGF.

bFGF (Trafermin; Kaken Pharmaceutical Co Ltd., Tokyo, Japan) has been clinically applied for the treatment of decubitus and dermal ulceration. However, bFGF has not yet been applied for the treatment of human IBD.

In this study, we first showed that rectal administration of hrbFGF had therapeutic effects in a DSS-induced colitis model. Indeed, hrbFGF recovered the decrease in body weight and histologically improved colitis. In our study, we confirmed that bFGF treatment did not yet improve DSS-induced colitis on day 8 (data not shown). In contrast, histologic analysis on day 11 revealed a significant improvement of DSS-induced colitis by bFGF treatment. Therefore, we consider that bFGF enhanced wound repair in the colonic tissues of mice with DSS-induced colitis rather than protected the colon against DSS-induced injury in this study.

In our preliminary study, intraperitoneal injection of hrbFGF (5.0 mg · kg^{-1} · day^{-1}) significantly improved body weight loss and colonic injury in a DSS-induced colitis model (data not shown). However, bFGF is considered to be rapidly cleared from the circulation, because the serum half-life of bFGF is reported to be 1.5–50 minutes after intravenous administration.[41–43] In addition, it was recently reported that rectal administration of EGF is effective for patients with active ulcerative colitis.[7] Moreover, systemic administration of bFGF might cause adverse effects, because bFGF mediates its biologic effects by binding to a variety of high-affinity cell-surface receptors, which are distributed not only in the colonic mucosa but also throughout the body.[44] Therefore, we considered that topical administration of bFGF might be more effective and less hazardous for the treatment of IBD than systemic administration, directly delivering bFGF to injured colonic mucosa.

Several mechanisms are considered for the improvement of colonic injury by bFGF. bFGF has been shown to stimulate proliferation of several intestinal cell lines.[22] We showed in this study that bFGF significantly increased the number of Ki-67–positive cells in the colonic epithelium of normal mice at 24 hours after bFGF treatment. Previous studies have shown that the increase of Ki-67–positive cell numbers directly correlates with crypt cell proliferation in the intestinal mucosa.[45–47] Interestingly, it was recently reported that exogenous bFGF markedly enhanced crypt stem cell survival in the mouse after radiation injury.[23] Vidrich reported that FGF receptor-3, whose ligand includes bFGF, was expressed prominently in the epithelial stem cell compartment.[48] Taken together, bFGF might enhance epithelial cell proliferation primarily through its direct effect on intestinal epithelial cells, including stem cells.

The present study clearly showed that TGF-β mRNA expression in the colonic tissues of normal mice was up-regulated after administration of bFGF. Moreover, we confirmed by enzyme-linked immunosorbent assay that bFGF increased TGF-β production in not only colonic epithelial cell lines but also fibroblast cell lines. Using an in vitro wounding model, Ciacci et al reported that TGF-β promotes cell migration, which does not require cell proliferation.[49] Moreover, Dignass et al showed that bFGF enhanced epithelial cell restitution through a TGF-β–dependent pathway in vitro.[22] In addition to cell proliferation, epithelial restitution is also known to play a significant role in the repair process of epithelial injury in the gastrointestinal tract.[3,4] Accordingly, TGF-β might be involved in the improvement of DSS-induced colitis by bFGF treatment through the enhancement of epithelial restitution. However, it may be noted that TGF-β is known to inhibit cell proliferation in epithelial cells. Thus, bFGF-induced TGF-β production also may be important in inhibiting unrestrained cell proliferation, as suggested previously.[22,50] Furthermore, because TGF-β is known to inhibit the production of proinflammatory cytokines, such as TNF-α and interferon gamma, in activated immune cells,[51] TGF-β may also have a role in down-regulation of inflammatory responses in DSS-induced colitis.

In this study, MUC2 and ITF gene expression in the colonic tissue of normal mice was up-regulated by treatment with bFGF. Moreover, the decreased mRNA expression of MUC2 and ITF in the colonic tissues of mice with DSS-induced colitis was recovered or even enhanced by bFGF treatment. Both MUC2 and ITF are predominantly expressed in the goblet cells of the small and large intestine.[52,53] Thus, the increase of MUC2 and ITF mRNA expression in the colonic tissues of mice with

DSS-induced colitis by bFGF treatment may have resulted from not only the direct effect of bFGF on those gene expressions but also recovery of goblet cell numbers. MUC2 is one of the secreted mucins and forms a gel-like mucus layer, which serves as a barrier to protect the intestinal epithelium from injurious luminal stimulants.[53] ITF promotes epithelial restitution after injury through epithelial cell migration.[54] Furthermore, several lines of evidence suggest that trefoil factors are involved in the stabilization of the mucus layer.[55,56] Taken together, it might be that bFGF has a role in enhancing mucosal barrier function not only by restoring injured epithelial structures but also by promoting mucus secretion and/or stabilization.

It may be noted in our study that although bFGF administration significantly reduced COX-2 gene expression in the colonic tissue of mice with DSS-induced colitis, it significantly enhanced COX-2 gene expression in normal colonic tissue. COX-2 is one of the key molecules involved in the mucosal repair process. Indeed, it has been shown that COX-2–mediated prostaglandin production contributes to the protection of colonic injury, the increase in crypt stem cell survival, the enhancement of angiogenesis, and the inhibition of proinflammatory cytokine production by activated macrophages.[57–62] Recently, Tessner et al reported that bFGF up-regulates COX-2 in human intestinal cell line I407,[63] and we obtained a similar stimulatory effect of bFGF on human colonic epithelial cell line Caco-2 (data not shown). Moreover, bFGF up-regulates COX-2 expression in endothelial cells, and COX-2 enhances bFGF-induced angiogenesis by stimulating VEGF gene expression.[64,65] In support of those data, the present study showed that hrbFGF significantly enhanced VEGF mRNA expression in the colonic tissues of normal mice. Taken together, therefore, bFGF appears to have a direct stimulatory action on COX-2 gene expression, which might result in the acceleration of mucosal repair in part through the induction of angiogenesis. However, our data also showed that gene expression of COX-2 and VEGF in the mice with hrbFGF-treated colitis was lower than in the nontreated mice with colitis in a dose-dependent manner. These discordant results were probably due to reduced inflammation in the colonic tissues of mice with DSS-induced colitis by the treatment with hrbFGF.

Zhao et al previously reported that costimulation with acidic FGF and anti-CD3 antibody activated $CD4^+$ T cells in vitro[66] and suggested an inflammatory effect of bFGF. In the present study, however, we did not find significant differences in the number of $CD4^+$ T cells or $CD4^+CD69^+$ T cells from MLN between mice with DSS-induced colitis with and without bFGF treatment. Moreover, the gene expression of anti-inflammatory molecules, such as IL-10 and PPAR-γ, in the colonic tissues of normal mice treated with bFGF was not influenced (data not shown). Thus, neither the number nor the function of immune-regulatory cells seemed to be affected by bFGF administration in our study.

In this study, we also examined the efficacy of bFGF on TNBS-induced colitis, a typical model of T cell–mediated colitis. Histologic analysis revealed that regeneration of colonic epithelium was enhanced by bFGF treatment, although bFGF treatment did not reduce lymphocytic infiltration in the colonic tissues of mice with TNBS-induced colitis. Additionally, the survival rate in the hrbFGF-treated group was significantly higher than in the nontreated group. Thus, bFGF could accelerate mucosal healing even in TNBS-induced colitis, mainly by promoting epithelial cell growth but not by exerting a direct anti-inflammatory effect on T cells.

In summary, our study suggests that rectal administration of bFGF is a promising option for the treatment of IBD. The safety of bFGF is already established because bFGF has been clinically applied to human diseases. A novel approach using bFGF might exert a synergistic effect with immune-regulatory agents for the treatment of IBD.

References

1. Fiocchi C. Inflammatory bowel disease: etiology and pathogenesis. Gastroenterology 1998;115:182–205.
2. Sartor RB. Intestinal microflora in human and experimental inflammation bowel disease. Curr Opin Gastroenterol 2001;17:324–330.
3. Goke M, Podolsky DK. Regulation of the mucosal epithelial barrier. Baillieres Clin Gastroenterol 1996;10:393–405.
4. Dignass AU. Mechanisms and modulation of intestinal epithelial repair. Inflamm Bowel Dis 2001;7:68–77.
5. Dignass AU, Sturm A. Peptide growth factors in the intestine. Eur J Gastroenterol Hepatol 2001;13:763–770.
6. Sandborn WJ, Sands BE, Wolf DC, Valentine JF, Safdi M, Katz S, Isaacs KL, Wruble LD, Katz J, Present DH, Loftus EV Jr, Graeme-Cook F, Odenheimer DJ, Hanauer SB. Repifermin (keratinocyte growth factor-2) for the treatment of active ulcerative colitis: a randomized, double-blind, placebo-controlled, dose-escalation trial. Aliment Pharmacol Ther 2003;17:1355–1364.
7. Sinha A, Nightingale J, West KP, Berlanga-Acosta J, Playford RJ. Epidermal growth factor enemas with oral mesalamine for mild-to-moderate left-sided ulcerative colitis or proctitis. N Engl J Med 2003;349:350–357.
8. Basilico C, Moscatelli D. The FGF family of growth factors and oncogenes. Adv Cancer Res 1992;59:115–165.
9. Schwartz SM, Liaw L. Growth control and morphogenesis in the development and pathology of arteries. J Cardiovasc Pharmacol 1993;21(Suppl 1):S31–S49.
10. Yanagisawa-Miwa A, Uchida Y, Nakamura F, Tomaru T, Kido H, Kamijo T, Sugimoto T, Kaji K, Utsuyama M, Kurashima C, et al. Salvage of infarcted myocardium by angiogenic action of basic fibroblast growth factor. Science 1992;257:1401–1403.
11. Harada K, Grossman W, Friedman M, Edelman ER, Prasad PV, Keighley CS, Manning WJ, Sellke FW, Simons M. Basic fibroblast

growth factor improves myocardial function in chronically ischemic porcine hearts. J Clin Invest 1994;94:623–630.
12. Bikfalvi A, Klein S, Pintucci G, Rifkin DB. Biological roles of fibroblast growth factor-2. Endocr Rev 1997;18:26–45.
13. Rieck P, Assouline M, Hartmann C, Pouliquen Y, Courtois Y. [Effect of recombinant human basic fibroblast growth factor (rh-bFGF) on wound healing of the corneal epithelium]. Ophthalmologe 1993;90:646–651.
14. Hoppenreijs VP, Pels E, Vrensen GF, Treffers WF. Basic fibroblast growth factor stimulates corneal endothelial cell growth and endothelial wound healing of human corneas. Invest Ophthalmol Vis Sci 1994;35:931–944.
15. Schuschereba ST, Bowman PD, Ferrando RE, Lund DJ, Quong JA, Vargas JA. Accelerated healing of laser-injured rabbit retina by basic fibroblast growth factor. Invest Ophthalmol Vis Sci 1994; 35:945–954.
16. Stenberg BD, Phillips LG, Hokanson JA, Heggers JP, Robson MC. Effect of bFGF on the inhibition of contraction caused by bacteria. J Surg Res 1991;50:47–50.
17. LeGrand EK, Burke JF, Costa DE, Kiorpes TC. Dose responsive effects of PDGF-BB, PDGF-AA, EGF, and bFGF on granulation tissue in a guinea pig partial thickness skin excision model. Growth Factors 1993;8:307–314.
18. Albertson S, Hummel RP III, Breeden M, Greenhalgh DG. PDGF and FGF reverse the healing impairment in protein-malnourished diabetic mice. Surgery 1993;114:368–372; discussion 372–373.
19. Nozaki K, Finklestein SP, Beal MF. Basic fibroblast growth factor protects against hypoxia-ischemia and NMDA neurotoxicity in neonatal rats. J Cereb Blood Flow Metab 1993;13:221–228.
20. Logan A, Berry M. Transforming growth factor-beta 1 and basic fibroblast growth factor in the injured CNS. Trends Pharmacol Sci 1993;14:337–342.
21. Ortega S, Ittmann M, Tsang SH, Ehrlich M, Basilico C. Neuronal defects and delayed wound healing in mice lacking fibroblast growth factor 2. Proc Natl Acad Sci U S A 1998;95:5672–5677.
22. Dignass AU, Tsunekawa S, Podolsky DK. Fibroblast growth factors modulate intestinal epithelial cell growth and migration. Gastroenterology 1994;106:1254–1262.
23. Houchen CW, George RJ, Sturmoski MA, Cohn SM. FGF-2 enhances intestinal stem cell survival and its expression is induced after radiation injury. Am J Physiol 1999;276:G249–G258.
24. Okayasu I, Hatakeyama S, Yamada M, Ohkusa T, Inagaki Y, Nakaya R. A novel method in the induction of reliable experimental acute and chronic ulcerative colitis in mice. Gastroenterology 1990;98:694–702.
25. Williams KL, Fuller CR, Dieleman LA, DaCosta CM, Haldeman KM, Sartor RB, Lund PK. Enhanced survival and mucosal repair after dextran sodium sulfate-induced colitis in transgenic mice that overexpress growth hormone. Gastroenterology 2001;120: 925–937.
26. Gibson UE, Heid CA, Williams PM. A novel method for real time quantitative RT-PCR. Genome Res 1996;6:995–1001.
27. Winer J, Jung CK, Shackel I, Williams PM. Development and validation of real-time quantitative reverse transcriptase-polymerase chain reaction for monitoring gene expression in cardiac myocytes in vitro. Anal Biochem 1999;270:41–49.
28. Neurath MF, Fuss I, Kelsall BL, Stuber E, Strober W. Antibodies to interleukin 12 abrogate established experimental colitis in mice. J Exp Med 1995;182:1281–1290.
29. Elson CO, Beagley KW, Sharmanov AT, Fujihashi K, Kiyono H, Tennyson GS, Cong Y, Black CA, Ridwan BW, McGhee JR. Hapten-induced model of murine inflammatory bowel disease: mucosa immune responses and protection by tolerance. J Immunol 1996;157:2174–2185.
30. Luck MS, Bass P. Effect of epidermal growth factor on experimental colitis in the rat. J Pharmacol Exp Ther 1993;264:984–990.
31. Procaccino F, Reinshagen M, Hoffmann P, Zeeh JM, Lakshmanan J, McRoberts JA, Patel A, French S, Eysselein VE. Protective effect of epidermal growth factor in an experimental model of colitis in rats. Gastroenterology 1994;107:12–17.
32. Egger B, Procaccino F, Sarosi I, Tolmos J, Buchler MW, Eysselein VE. Keratinocyte growth factor ameliorates dextran sodium sulfate colitis in mice. Dig Dis Sci 1999;44:836–844.
33. Byrne FR, Farrell CL, Aranda R, Rex KL, Scully S, Brown HL, Flores SA, Gu LH, Danilenko DM, Lacey DL, Ziegler TR, Senaldi G. rHuKGF ameliorates symptoms in DSS and CD4(+)CD45RB(Hi) T cell transfer mouse models of inflammatory bowel disease. Am J Physiol Gastrointest Liver Physiol 2002;282:G690–G701.
34. Miceli R, Hubert M, Santiago G, Yao DL, Coleman TA, Huddleston KA, Connolly K. Efficacy of keratinocyte growth factor-2 in dextran sulfate sodium-induced murine colitis. J Pharmacol Exp Ther 1999;290:464–471.
35. Han DS, Li F, Holt L, Connolly K, Hubert M, Miceli R, Okoye Z, Santiago G, Windle K, Wong E, Sartor RB. Keratinocyte growth factor-2 (FGF-10) promotes healing of experimental small intestinal ulceration in rats. Am J Physiol Gastrointest Liver Physiol 2000;279:G1011–G1022.
36. Jeffers M, McDonald WF, Chillakuru RA, Yang M, Nakase H, Deegler LL, Sylander ED, Rittman B, Bendele A, Sartor RB, Lichenstein HS. A novel human fibroblast growth factor treats experimental intestinal inflammation. Gastroenterology 2002;123:1151–1162.
37. Farrell CL, Rex KL, Chen JN, Bready JV, DiPalma CR, Kaufman SA, Rattan A, Scully S, Lacey DL. The effects of keratinocyte growth factor in preclinical models of mucositis. Cell Prolif 2002; 35(Suppl 1):78–85.
38. Meropol NJ, Somer RA, Gutheil J, Pelley RJ, Modiano MR, Rowinsky EK, Rothenberg ML, Redding SW, Serdar CM, Yao B, Heard R, Rosen LS. Randomized phase I trial of recombinant human keratinocyte growth factor plus chemotherapy: potential role as mucosal protectant. J Clin Oncol 2003;21:1452–1458.
39. Jimenez PA, Rampy MA. Keratinocyte growth factor-2 accelerates wound healing in incisional wounds. J Surg Res 1999;81:238–242.
40. Robson MC, Phillips TJ, Falanga V, Odenheimer DJ, Parish LC, Jensen JL, Steed DL. Randomized trial of topically applied repifermin (recombinant human keratinocyte growth factor-2) to accelerate wound healing in venous ulcers. Wound Repair Regen 2001;9:347–352.
41. Whalen GF, Shing Y, Folkman J. The fate of intravenously administered bFGF and the effect of heparin. Growth Factors 1989;1: 157–164.
42. Edelman ER, Nugent MA, Karnovsky MJ. Perivascular and intravenous administration of basic fibroblast growth factor: vascular and solid organ deposition. Proc Natl Acad Sci U S A 1993;90: 1513–1517.
43. Lazarous DF, Shou M, Stiber JA, Dadhania DM, Thirumurti V, Hodge E, Unger EF. Pharmacodynamics of basic fibroblast growth factor: route of administration determines myocardial and systemic distribution. Cardiovasc Res 1997;36:78–85.
44. Hughes SE. Differential expression of the fibroblast growth factor receptor (FGFR) multigene family in normal human adult tissues. J Histochem Cytochem 1997;45:1005–1019.
45. Gerdes J, Schwab U, Lemke H, Stein H. Production of a mouse monoclonal antibody reactive with a human nuclear antigen associated with cell proliferation. Int J Cancer 1983;31:13–20.
46. Johnston PG, O'Brien MJ, Dervan PA, Carney DN. Immunohistochemical analysis of cell kinetic parameters in colonic adenocarcinomas, adenomas, and normal mucosa. Hum Pathol 1989;20: 696–700.

47. Gerdes J, Lemke H, Baisch H, Wacker HH, Schwab U, Stein H. Cell cycle analysis of a cell proliferation-associated human nuclear antigen defined by the monoclonal antibody Ki-67. J Immunol 1984;133:1710–1715.
48. Vidrich A. Signaling through FGFR3 is neccesary for expansion of the epithelial stem cell compartment during normal intestinal development (abstr). Gastroenterology 2003;124:A22.
49. Ciacci C, Lind SE, Podolsky DK. Transforming growth factor beta regulation of migration in wounded rat intestinal epithelial monolayers. Gastroenterology 1993;105:93–101.
50. Suemori S, Ciacci C, Podolsky DK. Regulation of transforming growth factor expression in rat intestinal epithelial cell lines. J Clin Invest 1991;87:2216–2221.
51. Letterio JJ, Roberts AB. Regulation of immune responses by TGF-beta. Annu Rev Immunol 1998;16:137–161.
52. Wong WM, Poulsom R, Wright NA. Trefoil peptides. Gut 1999; 44:890–895.
53. Corfield AP, Myerscough N, Longman R, Sylvester P, Arul S, Pignatelli M. Mucins and mucosal protection in the gastrointestinal tract: new prospects for mucins in the pathology of gastrointestinal disease. Gut 2000;47:589–594.
54. Dignass A, Lynch-Devaney K, Kindon H, Thim L, Podolsky DK. Trefoil peptides promote epithelial migration through a transforming growth factor beta-independent pathway. J Clin Invest 1994; 94:376–383.
55. Kindon H, Pothoulakis C, Thim L, Lynch-Devaney K, Podolsky DK. Trefoil peptide protection of intestinal epithelial barrier function: cooperative interaction with mucin glycoprotein. Gastroenterology 1995;109:516–523.
56. Sands BE, Podolsky DK. The trefoil peptide family. Annu Rev Physiol 1996;58:253–273.
57. Tessner TG, Cohn SM, Schloemann S, Stenson WF. Prostaglandins prevent decreased epithelial cell proliferation associated with dextran sodium sulfate injury in mice. Gastroenterology 1998;115:874–882.
58. Morteau O, Morham SG, Sellon R, Dieleman LA, Langenbach R, Smithies O, Sartor RB. Impaired mucosal defense to acute colonic injury in mice lacking cyclooxygenase-1 or cyclooxygenase-2. J Clin Invest 2000;105:469–478.
59. Form DM, Auerbach R. PGE2 and angiogenesis. Proc Soc Exp Biol Med 1983;172:214–218.
60. Cohn SM, Schloemann S, Tessner T, Seibert K, Stenson WF. Crypt stem cell survival in the mouse intestinal epithelium is regulated by prostaglandins synthesized through cyclooxygenase-1. J Clin Invest 1997;99:1367–1379.
61. Knudsen PJ, Dinarello CA, Strom TB. Prostaglandins posttranscriptionally inhibit monocyte expression of interleukin 1 activity by increasing intracellular cyclic adenosine monophosphate. J Immunol 1986;137:3189–3194.
62. Marcinkiewicz J. In vitro cytokine release by activated murine peritoneal macrophages: role of prostaglandins in the differential regulation of tumor necrosis factor alpha, interleukin 1, and interleukin 6. Cytokine 1991;3:327–332.
63. Tessner TG, Muhale F, Schloemann S, Cohn SM, Morrison A, Stenson WF. Basic fibroblast growth factor upregulates cyclooxygenase-2 in I407 cells through p38 MAP kinase. Am J Physiol Gastrointest Liver Physiol 2003;284:G269–G279.
64. Kage K, Fujita N, Oh-hara T, Ogata E, Fujita T, Tsuruo T. Basic fibroblast growth factor induces cyclooxygenase-2 expression in endothelial cells derived from bone. Biochem Biophys Res Commun 1999;254:259–263.
65. Majima M, Hayashi I, Muramatsu M, Katada J, Yamashina S, Katori M. Cyclo-oxygenase-2 enhances basic fibroblast growth factor-induced angiogenesis through induction of vascular endothelial growth factor in rat sponge implants. Br J Pharmacol 2000;130:641–649.
66. Zhao XM, Byrd VM, McKeehan WL, Reich MB, Miller GG, Thomas JW. Costimulation of human CD4+ T cells by fibroblast growth factor-1 (acidic fibroblast growth factor). J Immunol 1995;155: 3904–3911.

Received March 15, 2004. Accepted December 22, 2004.

Address requests for reprints to: Kazuichi Okazaki, MD, PhD, Third Department of Internal Medicine, Kansai Medical University, 10-15 Fumizono-cho, Moriguchi City, Osaka, 570-8506, Japan. e-mail: okazaki@takii.kmu.ac.jp; fax: (81) 6-6996-4874.

Supported in part by the Establishment of International COE for Integration of Transplantation Therapy and Regenerative Medicine (COE program of the Ministry of Education, Culture, Sports, Science, and Technology, Japan); Grant-in-Aid for Scientific Research (C) from the Ministry of Culture and Science in Japan (16560645); and Health and Labour Science Research Grants from the Japanese Ministry of Health, Labour and Welfare, and Research on Measures for Intractable Disease (Inflammatory Bowel Disease).

Transforming Growth Factor (TGF)-β1–producing Regulatory T Cells Induce Smad-mediated Interleukin 10 Secretion That Facilitates Coordinated Immunoregulatory Activity and Amelioration of TGF-β1–mediated Fibrosis

Atsushi Kitani,[1] Ivan Fuss,[1] Kazuhiko Nakamura,[1] Fumiyuki Kumaki,[2] Takashi Usui,[1] and Warren Strober[1]

[1]*Mucosal Immunity Section, Laboratory of Clinical Investigation, National Institute of Allergy and Infectious Diseases, and* [2]*Laboratory of Pathology, National Lung, Heart, and Blood Institute, National Institutes of Health, Bethesda, MD 20892*

The Journal of Experimental Medicine

Abstract

Interleukin (IL)-10 and transforming growth factor (TGF)-β1 are suppressor cytokines that frequently occur together during a regulatory T cell response. Here we used a one gene doxycycline (Dox)-inducible plasmid encoding TGF-β1 to analyze this association and test its utility. In initial studies, we showed that intranasal administration of this plasmid (along with Dox) led to the appearance of TGF-β1–producing cells (in spleen and lamina propria) and the almost concomitant appearance of IL-10–producing cells. Moreover, we showed that these cells exert Dox-regulated suppression of the T helper cell (Th)1-mediated inflammation in trinitrobenzene sulfonic acid colitis. In subsequent in vitro studies using retroviral TGF-β1 expression, we established that IL-10 production by Th1 cells occurs after exposure to TGF-β1 from either an endogenous or exogenous source. In addition, using a self-inactivating retrovirus luciferase reporter construct we showed that TGF-β1 induces Smad4, which then binds to and activates the IL-10 promoter. Furthermore, intranasal TGF-β1 plasmid administration ameliorates bleomycin-induced fibrosis in wild-type but not IL-10–deficient mice, strongly suggesting that the amelioration is IL-10 dependent and that IL-10 protects mice from TGF-β1–mediated fibrosis. Taken together, these findings suggest that the induction of IL-10 by TGF-β1 is not fortuitous, but instead fulfills important requirements of TGF-β1 function after its secretion by regulatory T cells.

Key words: Th1 cells • trinitrobenzene sulfonic acid • fibrosis • doxycycline • transcription

Introduction

In recent years, evidence has accumulated indicating that naturally occurring regulatory cells producing TGF-β and/or IL-10 can prevent or even reverse Th1 cell–mediated inflammation (1–3). To take advantage of this finding for the treatment of Th1-mediated mucosal inflammation, we previously developed a method of creating "genetically engineered" regulatory cells in vivo by direct introduction of DNA encoding a regulatory cytokine, TGF-β1(4). In this method the TGF-β1–encoding DNA (in the form of a plasmid) is instilled into the nose and is either taken up by migrating cells in the nasal mucosa or by cells at distant sites exposed to plasmid that gains access to the circulation. In either case, cells (both T cells and macrophages) producing TGF-β1 can subsequently be found in the gastrointestinal tract, where they either prevent colitis caused by intrarectal administration of trinitrobenzene sulfonic acid (TNBS), or treat such colitis after it is established (5, 6). One unexpected finding arising from this method of inducing TGF-β1–producing cells is that at sites of inflammation, T cells producing large amounts of IL-10 are also found, and both cytokines participate in the regulatory effect. This observation is consonant with previous findings showing that TGF-β1 and IL-10 secretion tends to occur together at site of inflam-

Address correspondence to Warren Strober, Mucosal Immunity Section, Laboratory of Clinical Investigation, National Institute of Allergy and Infectious Diseases, National Institutes of Health, Building 10, Room 11N238, 10 Center Drive, Bethesda, MD 20892. Phone: (301) 496-6810; Fax: (301) 402-2240; email: wstrober@niaid.nih.gov

Abbreviations used in this paper: Dox, doxycycline; EMSA, electrophoretic mobility shift assay; GFP, green fluorescent protein; LP, lamina propria; SBE, Smad-binding element; TNBS, trinitrobenzene sulfonic acid.

mation (7–9). In this study, we sought to determine the molecular and cellular basis of this association and to examine its clinical consequences.

For this purpose, we developed a one gene/integrated doxycycline (Dox)-regulatable plasmid (10) that allows for the rapid up-regulation and down-regulation of TGF-β1 by in vivo Dox administration. We observed that cosecretion of IL-10 induced by plasmid is limited to T cells and macrophages and that transduced $CD4^+$ T cells, reminiscent of naturally occurring suppressor T cells, produce large amounts of IL-10 as a result of TGF-β1–induced Smad4-mediated transcriptional activation of the IL-10 promoter. Further, we found that TGF-β1 plasmid administration somewhat paradoxically reverses bleomycin-induced pulmonary fibrosis in wild-type mice and such reversal is IL-10 dependent because it does not occur in IL-10–deficient mice in whom the plasmid does not induce IL-10. This suggests that the association of TGF-β1 and IL-10 secretion has advantages not only in relation to immunologic suppression, but also in relation to the ability of TGF-β1 to mediate fibrosis (11).

Materials and Methods

Mice. Specific pathogen-free, 5–7-wk-old male SJL/J mice and C57BL/6 mice were obtained from the National Cancer Institute animal facility. IL-10–deficient mice were from Taconic.

Construction of pTet-On-TGF-β1. Porcine-active TGF-β1 cDNA (12) was subcloned into pSuperlinker 1180 (Amersham Biosciences) and then inserted into pRetro-On (CLONTECH Laboratories, Inc.). rtTA-TGF-β1 cDNA mini–CMV-TRE fragment was then inserted into the XhoI site of pCI (Promega) that had two SV40 poly(A) in opposite directions (see Fig. 1 a).

Intranasal Administration of Plasmid DNA and Induction of TGF-β1. We administered pTet-On-TGF-β1 intranasally (100 μg plasmid in 20 μl PBS/mouse). Starting the next day, Dox was administered for 5 d (500 μg in PBS, i.p./day/mouse).

Induction of TNBS Colitis and Culture of Lamina Propria (LP) Mononuclear Cells. We administered 2.5 mg TNBS (Sigma-Aldrich) dissolved in 45–50% ethanol per rectum (4–7). After mice were killed, we isolated LP mononuclear cells from colon (13) and cultured them in 24-well plates (10^6 cells/ml; Costar) with the stimulation of coated anti-CD3ε and soluble anti-CD28 (BD Biosciences) to assess IFN-γ and IL-10, and with the stimulation of IFN-γ and SAC (Calbiochem) to assess IL-12 production. Cytokine productions in the supernatants were determined by ELISA kits (Endogen; references 4 and 7). Culture in serum-free medium supplemented with 1% nutridoma-SP (Roche Molecular Biochemicals) was performed for TGF-β1 ELISA without acid treatment (Max TGF-β1 assay kit; Promega).

Bleomycin Treatment. C57BL/6J mice were anesthetized by i.p. injection of ketamine-HCl and xylazine-HCl. We induced pulmonary fibrosis by intratracheal instillation of 0.15 U bleomycin hydrochloride (Calbiochem) in 50 μl PBS using a 25-gauge bulb-end needle.

Histological Examination. The left lung of each mouse was first perfused in situ, inflated, and then fixed with 10% buffered formalin. Paraffin-embedded sections were stained by the Masson's trichrome method.

Collagen Assay. We harvested right lungs on days 14–21 after bleomycin treatment and homogenized them in 10 mg tissue/10 ml 0.5 M acetic acid containing 1 mg pepsin and incubated them for 24 h at 4°C with stirring. We determined lung collagen content by assaying total soluble collagen using the Sircol Collagen Assay kit (Biocolor; references 14 and 15). Sircol dye reagent is known to bind specifically to hydroxy proline, i.e., [Gly-X-Y]n helical structures of Types I–V collagens. Acid soluble Type I collagen supplied with kit was used to generate a standard curve.

TGF-β1 Retroviral Transfection of Primary T Cells. We inserted active TGF-β1 cDNA into pBMN-IRES–green fluorescent protein (GFP; provided by G. Nolan, Stanford University, Stanford, CA) and then transfected it into Phoenix-eco (American Type Culture Collection) to collect retroviral supernatants. We stimulated SJL/J spleen $CD4^+$ T cells purified by $CD4^+$ T cell–enriched columns (R&D Systems) with anti-CD3ε/anti-CD28 under the Th1 (rIL-12 and anti–IL-4 mAb) or Th2 (rIL-4 and anti–IL-12 mAb) conditions (15), or OVA-specific T cell lines with 100 μg/ml OVA and APC. After 24 h stimulation, we added retroviral supernatant in the presence of polybrene and IL-2, and spun it at 1,000 *g* for 90 min, followed by overnight incubation at 32°C, and then resumed culture at 37°C (16). Every 12 d, Th1- and Th2-polarizing cells were restimulated. In some experiments, 2 ng/ml rTGF-β1 (R&D Systems) was added every 3 d. We also transfected nonviral TGF-β1 plasmid into various cell lines using LipofectAMINE2000 (Invitrogen) or the electroporation method.

Intracellular Cytokine Staining. On day 7 after stimulation of αCD3/CD28, $CD4^+$ T cells were stimulated with 50 ng/ml PMA and 0.5 mM ionomycin for 6 h with monensin, and then washed and fixed with 4% formaldehyde, and processed for cytokine staining with PE–anti–IL-10 and/or APC–anti–IFN-γ mAb (BD Biosciences).

Preparation of Nuclear Protein Extracts and Electrophoretic Mobility Shift Assays (EMSAs). Jurkat cells stimulated with 5 ng/ml TGF-β1 for 1 h were lysed in ice-cold hypotonic buffer (10 mM Hepes, pH 7.9, 1.5 mM MgCl2, 10 mM KCl, 0.1 mM EDTA, pH 8.0, 0.1 mM EGTA, 1 mM DTT, 0.6% Nonidet P-40, proteinase inhibitor cocktail, sodium vanadate, and sodium fluoride). The lysates were centrifuged to obtain nuclei pellets that were then extracted with high salt nuclear extraction buffer (20 mM Hepes-KOH, pH 7.9, 1.2 mM MgCl2, 420 mM NaCl, 25% glycerol, 0.5 mM DTT, proteinase inhibitors, sodium vanadate, and sodium fluoride) as described. Binding reactions containing 10 μg nuclear extracts and 2 ng end-labeled oligonucleotides were performed for 20 min at room temperature in 15 μl binding buffer (20 mM Hepes, pH 7.9, 30 mM KCl, 4 mM MgCl 2, 0.1 mM EDTA, 0.8 mM NaPi, 20% glycerol, 4 mM spermidine, and 3 mg poly dI–dC; references 17 and 18). The probe sequences used for EMSA are: Smad-binding element (SBE) variant in IL-10 promoter, 5′-GGGAAGGTCCAGACATAATC-3′; specific competitor of SBE variant, 5′-CAGGGTGTCCAGACGGCCAC-3′; nonspecific competitor of SBE variant, 5′-GGGAAGTTTTA-GACATAATC-3′; wild-type SBE sequence, 5′-CAGGGT-GTCTAGACGGCCAC-3′; and specific competitor of wild-type SBE, 5′-AGAATCGTCTAGACATATCT-3′. Antibody supershift assay using anti-Smad4 (Santa Cruz Biotechnology, Inc.) was performed as previously described (18). Protein–DNA complexes were resolved in 4% polyacrylamide gels in 0.5X TBE.

Preparation of Self-inactivated Retrovector for IL-10 Promoter Luciferase Assay in Primary T Cells. A 1.37 kb murine IL-10 promoter region was prepared by PCR using 5′Xho primer (265–290) 5′-GCAGTTCTCGAGTCAATTCCATTC and NcoI primer (1637–1614, GenBank M84340) 5′-AGCCAGCCATG-GTGGAGCTCTCTT and ligated into pGL3-Basic vector

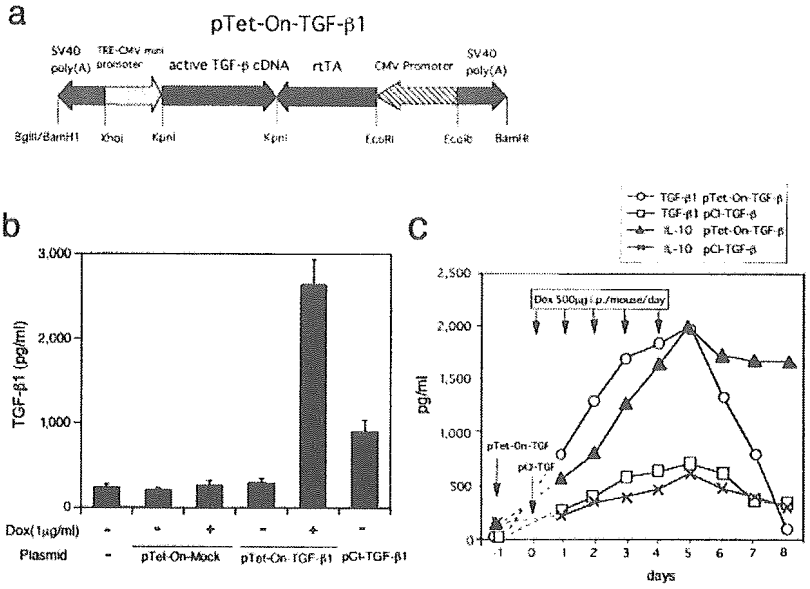

Figure 1. Active TGF-β expression in vitro and in vivo by pTet-On-TGF-β1. (a) Schematic map of the pTet-On-TGF-β1 construct. TRE, Tet-responsive element; rtTA, reverse tetracycline-controlled transactivator. (b) In vitro production of active TGF-β1 by Cos 7 cells transfected with pTet-On-TGF-β1 exhibited background TGF-β1 production in the absence of Dox and induced much greater amount of TGF-β1 than pCI-TGF-β1. (c) In vivo expression of active TGF-β1 and IL-10 in SJL/J mouse spleen cells after intranasal administration of pTet-On-TGF-β1 plasmid. Spleen cells from mice (n = 3) killed on the indicated days were cultured with anti-CD3/anti-CD28 in the absence of Dox and culture supernatants were assayed for active TGF-β1 and IL-10 by ELISA. Because Dox was not added to the splenocyte cultures, TGF-β1/IL-10 production measured reflect the capacity of cells to produce these cytokines in vivo. TGF-β1 and IL-10 production was rapidly induced by Dox in mice administered pTet-On-TGF-β. In addition, TGF-β1 but not IL-10 production rapidly declined after cessation of Dox.

(Promega). pBMN-IRES-EGFP was self-inactivated by converting the "TATA box" (AATAAA) in the 3′-LTR to the EcoRI GAATTC sequence (19) using a site-directed mutagenesis kit (Stratagene) with oligo 5′-CCCCGAGCTCGAATTCAGAGCCCAC-3′. IRES-EGFP fragment is replaced with two fragments: IL-10 promoter luciferase-DSE-U′-deleted SV40 polyA, which enables both polyadenylation and read through transcripts, and CMV promoter EGFP. Smad-binding sequence (726–733 in M84340) is mutated with the mutant SBE variant primer 5′-GTCCCTACTGAAGGGAAGTTTTAGACATAATCAAAGGACTACC-3′. Primary CD4 cells under Th1 or Th2 developing conditions were retrovirally infected and harvested on day 6. Cell lysates were analyzed for luciferase assays (Promega). All luciferase activities were normalized by the percentage of GFP expression by the flow cytometric analysis.

Results

Regulation of pTet-On-TGF-β1 In Vitro. As shown in Fig. 1 a, the regulatable "Tet-on" plasmid (termed pTet-On-TGF-β1) consisted of two expression units: a TGF-β1 cDNA that contains a mutation that results in production of "active" TGF-β1 (TGF-β1 not bound to latency-associated protein) under a mini-CMV promoter (12) and a CMV promoter-driven Tet-On transactivator (rtTA-VP16) that binds a Tet-responsive element after interaction with Dox (20, 21).

In initial studies, we transfected pTet-On-TGF-β1 into Cos 7 cells and showed that there was no expression of TGF-β1 in the absence of Dox. This is probably due to the fact that the two expression units are arrayed in the plasmid in opposite orientation so as to reciprocally block background transcription (22). In addition, as shown in Fig. 1 b, we observed that the transduced cells produce large amounts of TGF-β1 (2,600 pg/ml) in the presence of Dox, whereas cells transduced with a conventional unregulatable TGF-β1 expression plasmid (pCI-TGF-β1) secreted only moderate amounts of TGF-β1 (890 pg/ml).

Regulation of pTet-On-TGF-β1 In Vivo and Its Relation to IL-10 Secretion. In the next series of studies, we examined the in vivo expression and regulatability of TGF-β1 derived from pTet-On-TGF-β1 and its relation to IL-10 secretion. As shown in Fig. 1 c, we showed that after intranasal pTet-On-TGF-β1 administration accompanied by Dox coadministration, there was the rapid appearance of spleen cells secreting high amounts of TGF-β1 and the rapid disappearance of these cells after cessation of Dox administration. Perhaps more remarkably, we observed that the emergence of these TGF-β1–secreting cells was accompanied by the appearance of IL-10–producing cells, which then persisted after TGF-β1 secretion declined. These results clearly show that TGF-β1 secretion rapidly induces IL-10 secretion in vivo and that once such secretion is turned on it is not rapidly down-regulated as is the TGF-β1 secretion (which is under the control of a doxy-regulated promoter).

In a further study we investigated the ability of the Tet-On-TGF-β1 plasmid to affect an inflammatory state, exemplified by the Th1-type colitis induced by TNBS (4–7). Four groups of mice were studied: those receiving pTet-On-TGF-β1 with or without Dox and those receiving control plasmid (pTet-On-mock) also with or without Dox. As shown in Fig. 2 a, using body weight as an indicator of colitis, it was clear that the group that received pTet-On-TGF-β1 (i.n.) and Dox (i.p.) was protected from developing colitis, whereas the group receiving the plasmid in the absence of Dox (or those mice receiving pTet-ON-mock again with and without Dox) developed colitis. In addition, although LP cells from all three groups developing colitis produced large amounts of IL-12 and IFN-γ and small amounts of TGF-β1, LP cells from mice prevented from developing colitis produced small amounts of IL-12 and IFN-γ and very large amounts of TGF-β1 (Fig. 2 b). Of interest, the latter was much greater than that produced by cells taken from mice without inflamma-

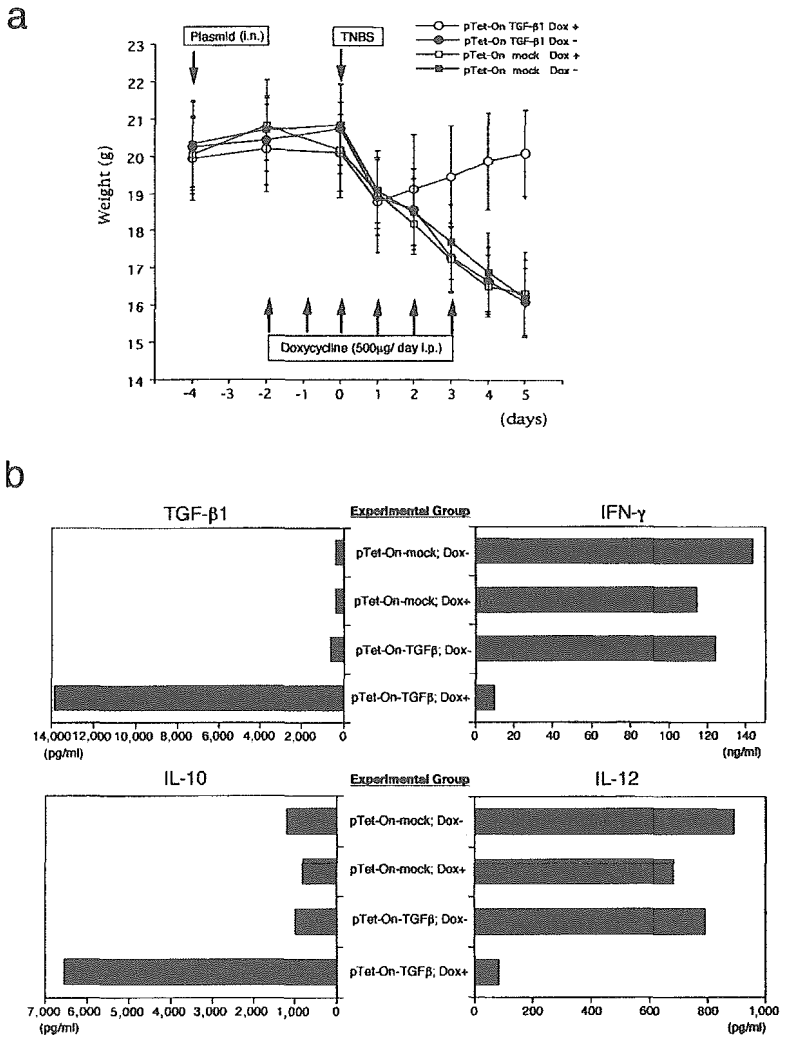

Figure 2. Effect of intranasal pTet-On-TGF-β1 administration on TNBS-induced colitis. (a) Weight changes of mice groups administered intrarectal TNBS and intranasal pTet-On-TGF-β or pTet-On-mock (control plasmid) with or without Dox (i.p.) Each group, n = 10. (b) LP cells from mice 5 d after TNBS colitis induction were stimulated and cultured for ELISA assays of TGF-β1, IFN-γ, IL-10, and IL-12. As shown, LP cells from mice administered Dox plus pTet-On-TGF-β1 produced large amounts of TGF-β1 and IL-10 and exhibited suppressed IL-12 and IFN-γ production. Data shown is representative of three independent experiments.

tion, reflecting the activation of the CMV promoter in an inflammatory milieu. In addition, LP cells from this group, but not those from the groups in which the plasmid was not accompanied by Dox administration, produced large amounts of IL-10. Thus, it was obvious that such IL-10 secretion was due to plasmid-induced TGF-β1 and not simply to the presence of a Th1 inflammation. In further studies not shown, we found that intranasal administration of pTet-On-TGF-β1 also reversed TNBS colitis after inflammation was established, but only in the presence of concomitant Dox administration.

Cell Types Producing IL-10 in Response to TGF-β1. Next, we defined the cell types capable of producing IL-10 in response to exposure to TGF-β1. Here we first transfected various murine cell lines with pCI-TGF-β1 under optimal conditions or, in the case of $CD4^+$ T cells that exhibit low transfection efficiency, we infected the cells with a retrovirus encoding TGF-β1 (see below). We then determined IL-10 production in the modified cells. As shown in Table I, a Th1 $CD4^+$ cell line (OVA-3), i.e., a T cell line maintained by repeated OVA plus APC stimulation for >6 wk, and two macrophage cell lines (RAW264 and MH-S) secreted substantial amounts of IL-10 after transfection (or infection). In contrast, a thymus-derived T cell (EL-4) as well as epithelial, squamous, and fibroblast cell lines from lung and other tissues did not produce IL-10 after transfection (although they did produce TGF-β1). These studies indicate that only certain types of hematopoietic cells are capable of IL-10 secretion as a result of exposure to TGF-β1.

IL-10 Production by Polarized Th1 Cell Populations in Response to Both Endogenous and Exogenous TGF-β1. Next, we addressed the question of whether the production of IL-10 in a Th1 milieu could arise from the Th1 cells themselves. To this end, we transduced naive $CD4^+$ T cells stimulated with anti-CD3/anti-CD28 with a bicistronic retroviral vector expressing both TGF-β and GFP (termed pBMN-TGF-β1 or retro-TGF-β1) under Th1 priming conditions (IL-12 and anti–IL-4) or Th2 priming conditions (IL-4 and anti–IL-12; reference 16). This allowed us to distinguish infected cells (GFP^+, TGF-β1–producing cells) from uninfected cells (GFP^-, TGF-β1–nonproducing cells). As shown in Fig. 3 a, although developing $CD4^+$ Th1 cells infected with control retrovirus (pBMN-mock or retro-mock, i.e., retrovirus encoding only GFP) did not